AN ABSTRACT OF THE THESIS OF

Edmund Jui-Ching Hsieh (Name) for the Ph.D. (Degree) in Electrical Engineering (Major)

Date thesis is presented March 18, 1966

Title THIN-FILM WIDEBAND TUNNEL-DIODE AMPLIFIER

Abstract approved [redacted] (Major professor)

Wideband tunnel-diode amplifiers using common-base transistor stages for isolation were investigated for stability criteria, frequency response, and the effects of temperature and voltage supply fluctuations. For the first time the full frequency spectrum of a tunnel-diode, from d-c to the gigahertz (GHz) range, was able to be utilized in an amplifier. Three experimental circuits constructed by conventional as well as thin-film techniques were tested. They represented a workable model of a new design of a tunnel-diode amplifier capable of having constant gain over a frequency spectrum from d-c to one-half GHz. It was shown that this design principle could be applied to extend the upper frequency limit to a few GHz if higher frequency tunnel-diodes and better circuit construction techniques are employed.

THIN-FILM WIDEBAND TUNNEL-DIODE AMPLIFIER

by

EDMUND JUI-CHING HSIEH

A THESIS

submitted to

OREGON STATE UNIVERSITY

in partial fulfillment of
the requirements for the
degree of

DOCTOR OF PHILOSOPHY

June 1966

APPROVED:

[redacted]

Assistant Professor of Electrical Engineering
In Charge of Major

[redacted]

Head of Electrical and Electronics Engineering Department

[redacted]

Dean of Graduate School

Date thesis is presented 3-18-66

Typed by Erma McClanathan

ACKNOWLEDGMENT

The writer is indebted to Professor James C. Looney for suggesting the problem and for guidance during the research. Thanks also go to Professor Louis N. Stone for his criticism and help in editing the manuscript.

Appreciation is extended to Mrs. Sidonie Warne who did the lettering in the photographs.

The project was initially financed by Tektronix, Inc. The masks used for the film depositions were made in the Tektronix laboratory. Their continuing interest and support of the project is sincerely appreciated.

TABLE OF CONTENTS

I. Introduction..... 1

II. Design and Theoretical Analysis..... 6

Amplifying Characteristics of the Tunnel-Diode..... 6

Circuit Considerations..... 10
Stability Criteria..... 10
Circuit Configuration of the Tunnel-Diode Amplifier..... 11
Operation Principles..... 14

Stability and Gain Analysis..... 15
A-C and D-C Loads on the Tunnel-Diode.. 15
Equivalent Circuits..... 17
Stability and Gain of a One-Stage Amplifier..... 20

Effects of Temperature and Voltage Supply Variations..... 25
Allowable Variation in g..... 25
Tolerance on Voltage Supply Variation.. 27
Tolerance on Temperature Variation..... 30

Examples of Practical Design..... 33

III. Experimental Results and Conclusion..... 42

The Construction of the Amplifiers..... 42
Conventional Circuit..... 42
Thin-Film Hybrid Circuits..... 42

Estimation of Circuit Parameters..... 44

Operation of the Amplifier..... 48
Adjustment on the Input Transistor T1.. 48
Adjustment on the Output Transistor T2. 48
Adjustment on R_2..... 50

Experimental Results and Conclusion..... 52
Experimental Results..... 52
Conclusion..... 63

Bibliography..... 65

Appendix..... 68

LIST OF FIGURES

Figure		
1	Characteristic of a Tunnel-Diode	6
2	Simple Series Circuit with Tunnel-Diode	7
3	Illustration of Stable Bias Condition at the Negative-Resistance Region	8
4	Illustration of Amplifying Characteristic of a Tunnel-Diode	9
5	Basic Elements of the Amplifying Circuit	12
6	Circuit Diagram of the One-Stage Amplifier	13
7	A-C Equivalent Load on the Tunnel-Diode	16
8	Equivalent Circuit of a Tunnel-Diode	18
9	Simplified Equivalent Circuit for the Emitter-Base Junction of a Transistor	19
10	Simplified Equivalent Circuit for the Collector Junction of a Transistor	20
11	Equivalent Circuit for Stability and Gain Analysis	21
12	Current Gain Versus Allowable Variations in g and Temperature	27
13	Effect of B^+ on the Operating Point of the Tunnel-Diode	28
14	One-Stage Amplifier, Conventional Circuit	35
15	One-Stage Thin-Film Amplifiers II and III (in Bracket)	36
16	Two-Stage Thin-Film Amplifiers IV and V (in Bracket)	37
17	Calculated Frequency Responses of the Amplifiers	40
18	Final Configuration of the Conventional Circuit Amplifier	43
19	Two-Stage Thin-Film Hybrid Amplifier	44

Figure

20 Experimental Circuit for Measuring the Emitter-Base Impedance..... 46

21 Emitter-Base Impedance Measurement Scheme.... 47

22 Graphical Analysis of the Operating Point of a Tunnel-Diode..... 50

23 Voltage-Current Characteristics of R_2..... 51

24 Block Diagram for the Testing of Amplifier Frequency Response..... 53

25 Output Responses with "+" and "-" Input Pulses of 120 ns Duration, Amplifier I..... 56

26 Output Responses with "+" and "-" Input Pulses of 20 ns Duration, Amplifier I..... 56

27 Risetimes of Input and Output, Amplifier I... 57

28 Frequency Response of Amplifier II..... 57

29 Output Responses with "+" and "-" Input Pulses of 120 ns Duration, Amplifier IV..... 58

30 Risetime of Amplifier IV..... 58

31 Possible Operating Points of Tunnel-Diode.... 59

32 Symmetrical Gains with "+" and "-" Inputs, Amplifier I..... 60

33 Risetimes with "+" and "-" Input Pulses, Amplifier I..... 60

34 Variation of Gain with Temperature, Amplifier I..... 62

35 Variation of Gain with Input Magnitude, Amplifier I..... 62

36 Masks Used for Thin-Film Depositions..... 69

37 Chamber Layout for Thin-Film Depositions..... 70

38 Completed Thin-Film Circuit Board for Two-Stage Amplifier..... 74

39 Close-Up of the Two-Stage Thin-Film Hybrid Amplifier..... 74

LIST OF TABLES

Table		
I	Pertinent Data of Transistors and Tunnel-Diodes	38
II	Estimated Values of the Amplifier's Equivalent Circuits	39
III	Summarized Results on the Frequency Responses of the Experimental Amplifiers	55
IV	Data on the Construction of the Thin-Film Circuit	72

THIN-FILM WIDEBAND TUNNEL-DIODE AMPLIFIER

I. INTRODUCTION

A considerable number of tunnel-diode amplifiers operating in the megahertz (MHz) and gigahertz (GHz) have been reported in the literature (2,20,29). Though some of them achieved a gain-bandwidth product of a few GHz, or even tens of GHz, few attained a bandwidth[1] higher than a decade (20,21) and hardly any showed promise of being able to develop into a truly wideband amplifier. This limitation on the bandwidth of the existing tunnel-diode amplifiers can be attributed only to the mode of the amplifier design and not to the tunnel-diode itself which is capable of operating from d-c to tens of GHz. The amplifier to be presented here does not have those inherent limitations on bandwidth and, for the first time, the full frequency capability of a tunnel-diode is utilized.

In this paper, the design and experimental results obtained with three models of a wideband and constant gain tunnel-diode amplifier designed for operation from

---

[1] The term bandwidth is defined as either, (1) the difference between the limiting frequencies of a continuous frequency band, or, (2) the range of frequencies within which performance falls within specific limits with respect to some characteristic. When the latter definition is adopted, the range can be expressed in terms of the ratio between the upper and lower limiting frequencies.

d-c to 500 MHz range will be presented. The current gain per stage of the amplifier was approximately three. More than one amplifier stage could be coupled together to obtain higher gain. The amplifiers were designed to work with a source impedance of 50 ohms and an input signal of five millivolts (mv).

The wide bandwidth was achieved by the use of common-base transistor stages to isolate the input and output load from the tunnel-diode. This assured the proper load impedance on the tunnel-diode for a wide frequency spectrum. Further, the isolation transistor stages also offered the means of coupling more than one amplifier stage together to attain even higher gain-bandwidth product. Thin-film circuitry was employed in the construction of the amplifiers to minimize the stray reactances, mainly inductances, due to the interconnections. The ultimate limitation for high-frequency operation will be the transistor's ability to maintain the isolation function and the inductances introduced by the interconnecting leads and by the emitter-base junction of the transistor. It was shown that the upper frequency limit will be in the few GHz range.

The main difficulties encountered in the design of tunnel-diode amplifiers for wideband operation were concerned essentially with questions of matching the

negative resistance of the tunnel-diode to the corresponding load impedance for an indicated frequency band and (at the same time) maintaining isolation between the input and output in order to obtain unidirectional gain. Being a two-terminal device, a tunnel-diode has 100% coupling between its input and output. If useful gain is to be obtained, this must be secured by additional circuit components.

The load-matching problem of the tunnel-diode amplifiers has usually been solved by the introduction of a resonant circuit (4,9,30). For the series resonant amplifier, the inserted inductance and the capacitance of the tunnel-diode formed a resonant circuit which can be tuned to a desired frequency. Similar to the other types of resonant amplifiers, wider bandwidth can be obtained at the expense of gain. A parallel configuration can also be realized for this type of amplifier by the use of a cavity resonator with a tuning coaxial capacitance bar (27). In amplifiers designed to operate at ultra-high frequencies, improvement of bandwidth can be achieved by employing band filters in the form of strip lines instead of tuning the resonant circuit to a fixed frequency (21).

The problem of obtaining unidirectional gain and/or isolation between input and output was resolved by

utilizing the reflection property of electromagnetic waves. Basically, the reflection-type amplifiers were designed so that the reflected signal from the amplifier would be constructive where gain was to be obtained and destructive where isolation was desired. One of the more popular reflection-type amplifiers called for a circulator to be used in the circuit (34). The input signal was fed to the tunnel-diode amplifier through the circulator which was usually made up of ferrite material and had the property of transmitting the electromagnetic wave through in only one direction. The amplified signal was reflected to the circulator, which directed it towards the load. With the impedances properly adjusted, the reflected wave was greater than the incident wave and thus power gain was obtained. The application of a circulator was, to some degree, limited to the centimeter waveband. At lower frequency (UHF), the dimensions of the circulator might prove to be excessively large and thus impractical.

Another method permitting directional transmission of the input signal was to use a 3-db coupler, or a hybrid junction (29). Two tunnel-diode amplifiers, connected to the junction with wave-guides differing in length by one-fourth of the operated wave-length, were employed in this configuration. This phase relationship resulted in the addition of the two amplified and

reflected waves at the output load, and cancellation at the input terminals. Theoretically, 100% addition or cancellation will take place for a single frequency only.

The schemes employed, as mentioned in the previous paragraphs, to obtain "useful gain" from tunnel-diode amplifiers were inherently frequency limited. It was obvious that a tuned circuit would have a limited bandwidth. The band-filters, circulators and hybrid coupled junctions were all designed for a specific frequency band. This was why most of the tunnel-diode amplifiers reported had a bandwidth less than a decade.

This paper presents a new approach for designing a wideband tunnel-diode amplifier. Only the circuit aspects of a tunnel-diode as a negative resistance amplifying component are included here. A discussion on the physics of tunnel-diodes can be found in other references (11,19,25). The paper begins with a discussion on the amplifying properties of tunnel-diodes when operated in the negative resistance region and then follows with a theoretical analysis of the amplifier design. The experimental results obtained from the three amplifiers constructed are reported in the last chapter.

II. DESIGN AND THEORETICAL ANALYSIS

Amplifying Characteristics of the Tunnel-Diode

One way of showing the reason why the tunnel-diode, being a two-terminal device and thus void of impedance transfer characteristic, can be used as an amplifier element is to examine its differential conductance as a function of the bias voltage (26, p. 3-22). Figure 1 shows the V-I characteristic of a tunnel-diode and its differential conductance g as a function of voltage.

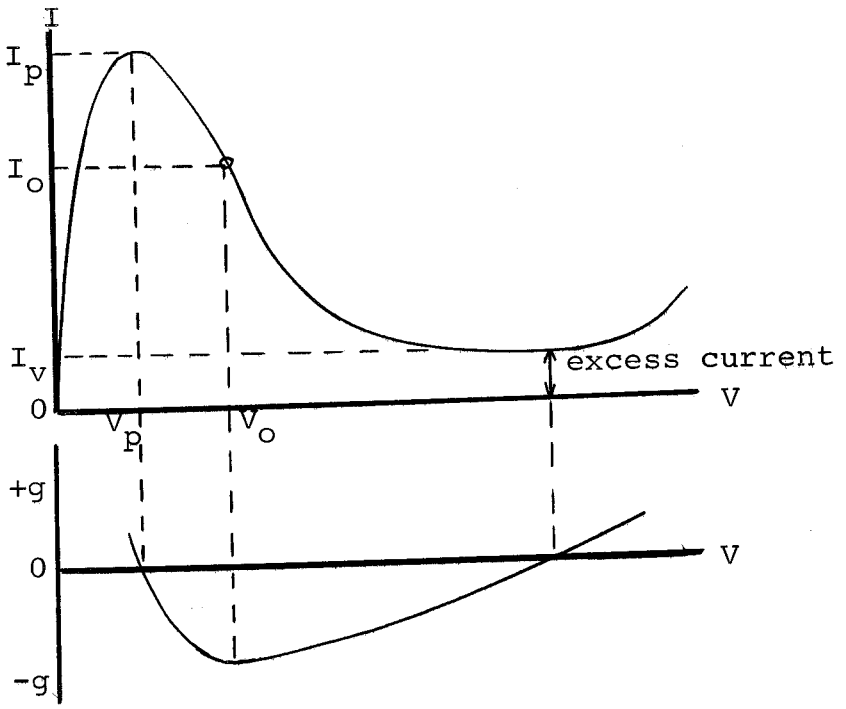

Figure 1. Characteristic of a tunnel-diode.

The most interesting feature in the characteristic curve is that the slope becomes negative, which yields negative values for g, for a certain range of bias voltage. A negative differential conductance, being opposite to the conventional positive conductance which consumes energy, implies the amplification of signal energy. This can be shown analytically. Consider the simple series circuit shown in Figure 2.

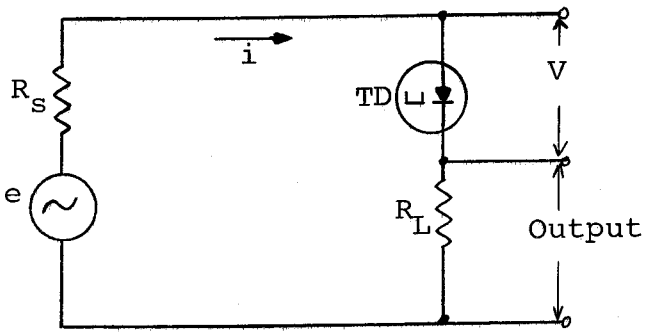

Figure 2. Simple series circuit with tunnel-diode.

The energy-balance equation of this series circuit is

$$ei = i^2R_s + i^2R_L + i^2r_d(V).$$

The differential resistance $r_d(V)$ of the tunnel-diode is a function of the d-c bias voltage, V. For the small signal case, r_d can be considered to have a constant value. When the tunnel-diode is biased at the negative-resistance region, at V_o as shown in Figure 3, r_d will be negative, causing the quantity i^2r_d to be negative also. By conventional circuit rules, negative power dissipation will be equivalent to power generation. The power "generated" is divided between the source resistance, R_s, and

the output load, R_L, and amplification results.

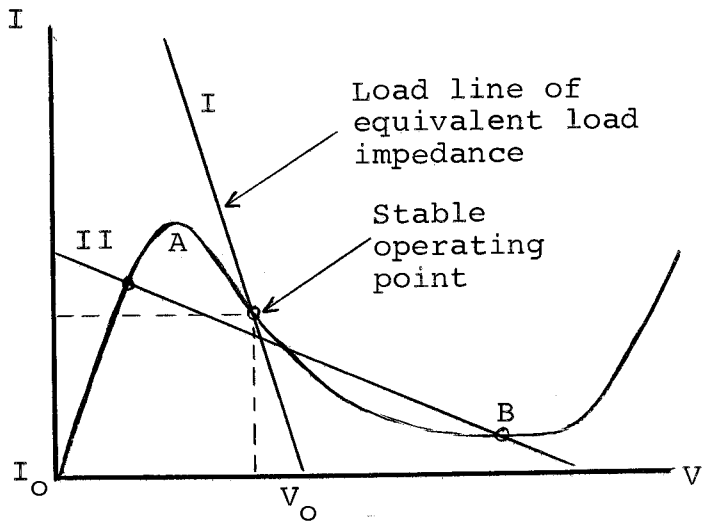

Figure 3. Illustration of stable bias condition at the negative-resistance region.

The source of this "generated" a-c power, from the principle of conservation of energy, can be traced to the d-c power supply. This becomes obvious when the total power dissipation of the tunnel-diode is considered,

$$p_{TD} = I_o V_o + i^2 r_d.$$

When the tunnel-diode is operated in the negative-resistance region (V_o, I_o), the power dissipation p_{TD} will be decreased by an amount $i^2 r_d$ from the quiescent value $I_o V_o$; and the same amount, as shown previously, will appear in part at the output load. In other words, the tunnel-diode, when operated in the negative-resistance region, can convert the d-c source energy into

signal energy.

The amplification of signal energy can also be illustrated graphically. Consider a simple circuit where a tunnel-diode is shunted by a load resistor R. When the value of R is properly chosen (1/R is slightly larger than $|-g|$), a composite V-I characteristic such as shown in Figure 4 can be obtained.

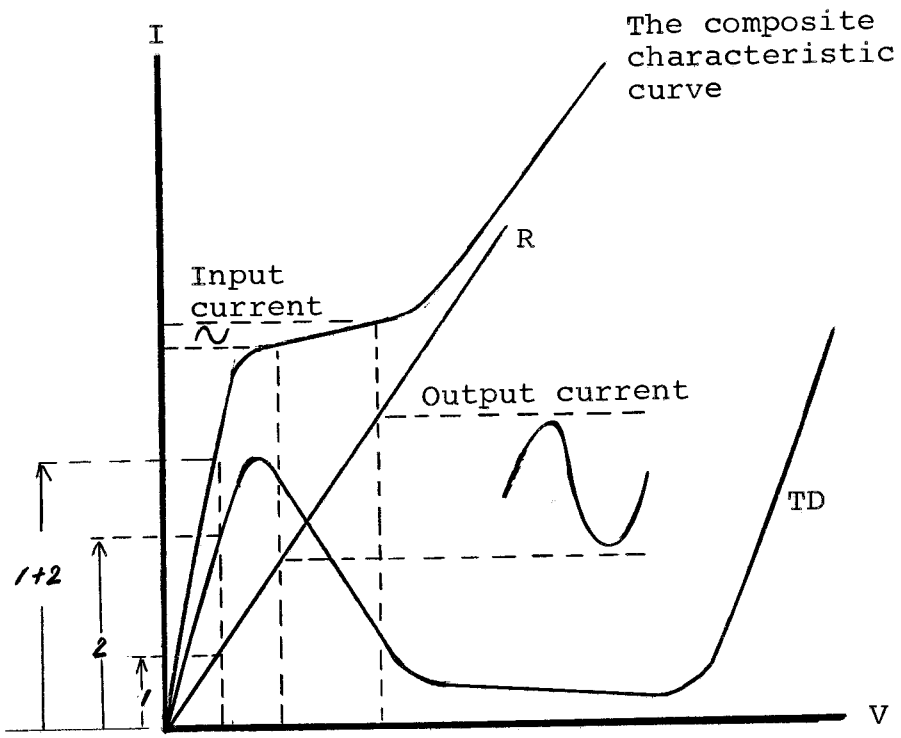

Figure 4. Illustration of amplifying characteristic of a tunnel-diode.

A small incoming signal current, which is represented by the current swing in the composite characteristic curve, will cause a much larger current swing at the load resistor R and amplification results.

Circuit Considerations

Stability Criteria

As already shown, amplification with tunnel-diodes is possible when the operating point is in the negative-resistance portion of the tunnel-diode characteristic. However, this operating point will be stable only under certain conditions. The subject of this stability criteria has been discussed quite thoroughly by Hines (18) and others (3,10,24,32). Generalized stability criteria have been established for many loading conditions (7,12,15,28). The most important criteria is that, for all frequencies where gain is larger than one, the equivalent load impedance evaluated in parallel with the tunnel-diode, should always be less than the absolute value of the negative-resistance ($|-r_d|$) of the tunnel-diode at the operating point. The requirement can be clearly illustrated by drawing different load lines (for various equivalent load impedances) in the negative-resistance portion of the tunnel-diode characteristic curve (see Figure 3). If the load line is to intercept the negative-resistance region of the characteristic curve at a single point and a single point only, as shown by load line I in Figure 3, the slope of the load line (which equals the negative of the reciprocal of the load impedance) must be greater than that of the

negative slope of the tunnel-diode characteristic curve. In other words, to have stable operation the equivalent impedance must be less than the negative resistance of the tunnel-diode. This requirement imposes certain specific conditions on the method of coupling the input signal and output load to the tunnel-diode, on the choice of bias source, and the method whereby it is connected.

If the equivalent load impedance is larger than the negative resistance of the tunnel-diode, the load line will intercept at more than one point with the tunnel-diode curve, as shown by load line II in Figure 3. Under this condition the operating point will be switching between A and B and amplification will be impossible.

Circuit Configuration of the Tunnel-Diode Amplifier

The main feature in the following circuit design is that the input and output are isolated from the tunnel-diode by common-base transistor stages. Therefore, there is more freedom in selecting the proper loading on the tunnel-diode to achieve the desired gain and bandwidth, and meet the stability requirement for all frequencies. The circuit that will perform the function just mentioned takes the form as shown in Figure 5.

Figure 5 includes only the main part of the tunnel-diode amplifier. To bias the tunnel-diode and transistors at the proper operating points, additional

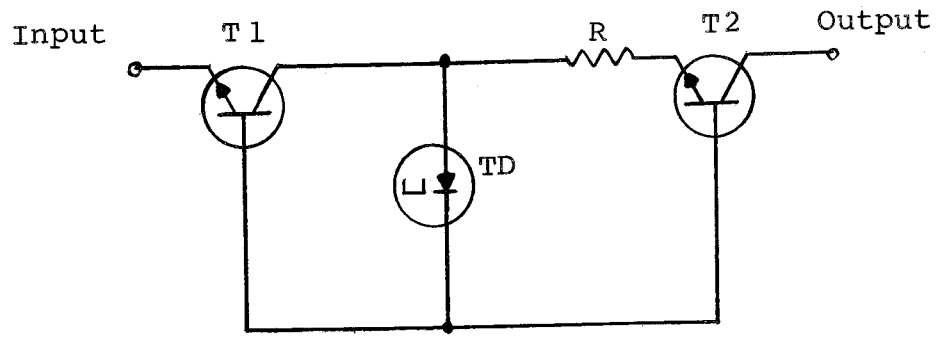

Figure 5. Basic elements of the amplifying circuit.

circuitry is required. With the added circuitry, the complete one-stage tunnel-diode amplifier design is as shown in Figure 6.

A brief list of symbols used in the circuit diagram will be helpful in the discussion of circuit features that follows.

List of Symbols Used in the Circuit Diagram

B^+ and B^- ...	voltage supplies, above and below ground respectively
C_1, C_2	capacitors used for a-c ground
D1, D2	diodes
R_A, R_B	resistors involved in d-c biasing
R_1, R_2	resistors involved in the a-c and d-c loading
T1 and T2 ...	input and output transistors for isolation purpose
TD	tunnel-diode
ZD	zener diode

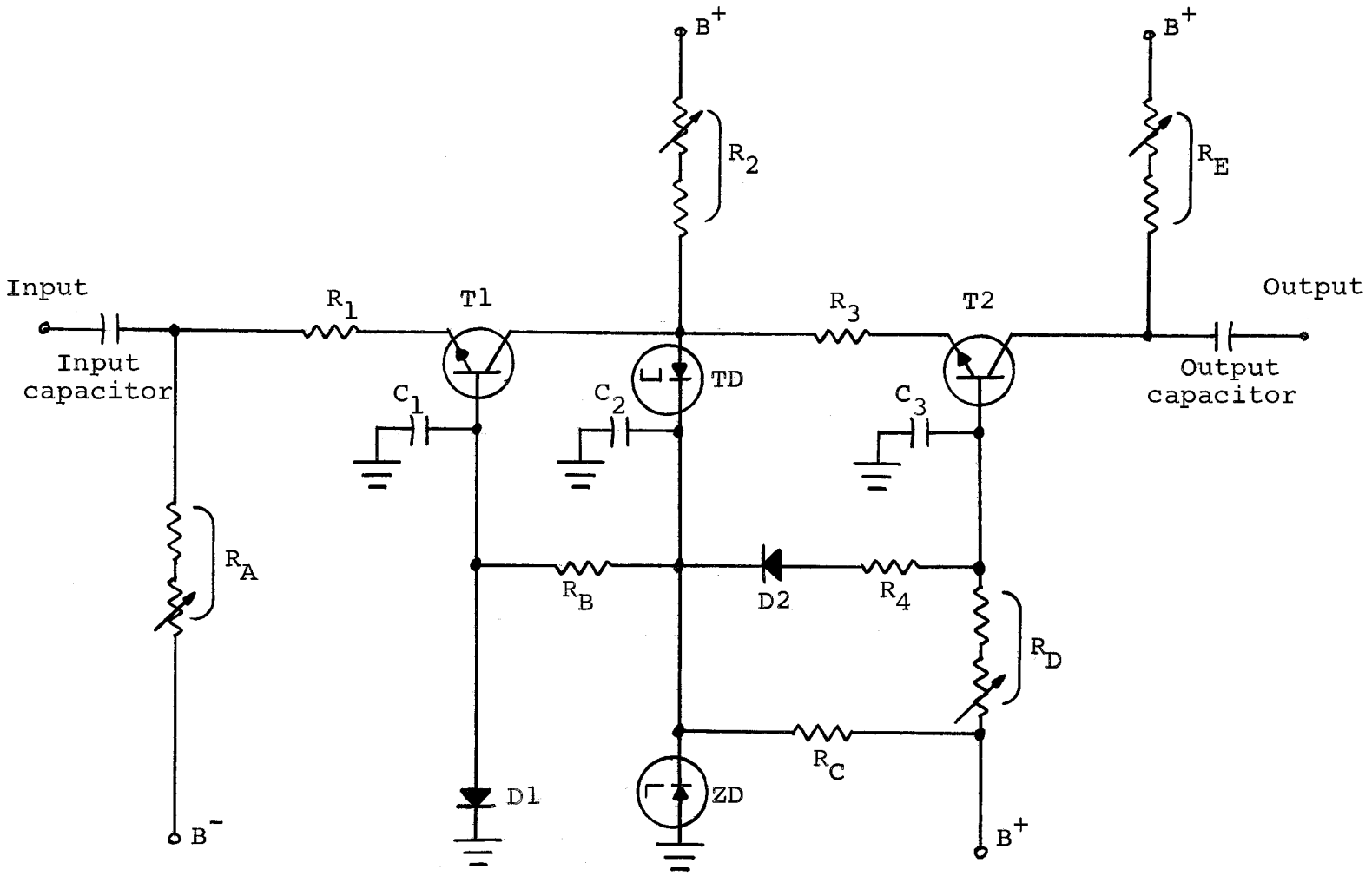

Figure 6. Circuit diagram of the one-stage amplifier.

Operation Principles

With reference to Figure 5, the input current, after passing through T1, encounters the tunnel-diode and its parallel load impedance. With the components properly chosen, a composite V-I characteristic similar to that shown in Figure 4 can be obtained. The amplified input current at the emitter circuit of T2 will appear at the output and current gain is achieved.

The additional circuitry shown in Figure 6 is mainly for the purpose of d-c biasing and impedance matching. R_A controls the operating point of T1, and R_1 is added to give the proper impedance matching with the signal source. D1 and ZD serve as d-c voltage references which will not be affected by the signal voltage or current. The operating point of T2 is set by R_D. With R_2 controlling the d-c bias current, the operating point of the tunnel-diode will depend on R_2 as well as the current in T1 and T2. Normally, currents in T1 and T2 are approximately the same so that the tunnel-diode's biasing point will be very sensitive to the value of R_2. Another mode of operation is that T2 will be operated around the cut-off region so that its emitter-base impedance, Z_{eb}, can be used as an adjustable load on the tunnel-diode. Under this condition, the d-c currents in T1 and TD will be drawn from the source through R_2. The gain of the

amplifier can be adjusted by varying the load applied to the tunnel-diode.

Stability and Gain Analysis

A-C and D-C Loads on the Tunnel-Diode

The value of the load impedance of the tunnel-diode changes with frequency. For stable operation, the stability criteria should be satisfied at the low frequency end, d-c, as well as at any other frequency. In general the d-c and a-c loads are different in an amplifier. However, in order to have a flat gain throughout the operating frequency range, the a-c and d-c loads should be kept approximately the same.

The a-c load will be discussed first. Assume that the capacitors C_1 to C_3 are large enough to become effective a-c short-circuits to ground, and the transistors T1 and T2 offer sufficient isolation;[2] the a-c equivalent load on the tunnel-diode will be as shown in Figure 7.

There are three impedances, the collector-base inpedance of T1, $\left[Z_{cb}\right]_{T1}$, R_2 and the sum of R_3 and

---

[2] It is implied here, as well as in the discussions throughout the theoretical analysis, that the operating frequency in question is always below the upper cutoff frequencies of the active components concerned.

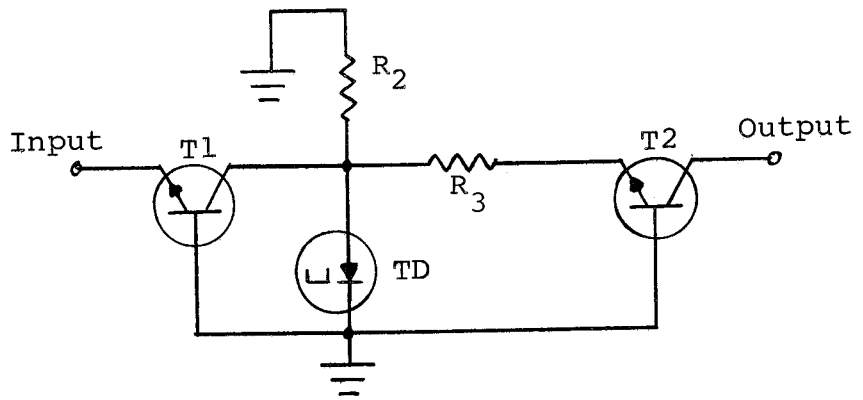

Figure 7. A-C equivalent load on the tunnel-diode.

emitter-base impedance of T2, $\left[Z_{eb}\right]_{T2}$, which shunt across the tunnel-diode. With R_2 and $\left[Z_{cb}\right]_{T1}$ in the order of kilo-ohms, the a-c load on the tunnel-diode will be

$$\left[Z\right]_{a\text{-}c} = R_3 + \left[Z_{eb}\right]_{T2}.$$

When T2 is biased in the active region, $\left[Z_{eb}\right]_{T2}$ will have the value of a few ohms. This leaves R_3 to be the determining factor in the loading.

The d-c load is more complicated. A significant portion of the circuitry is devoted to satisfy the d-c stability requirements. D2 and R_4 are added to provide a d-c return path for the effective a-c load $\left[Z\right]_{a\text{-}c}$. The resistance of this d-c return path must be kept at a minimum so that the difference between a-c and d-c load will be small. The choice of D2 depends on the potential difference between the base of T2 and the cathode of the

tunnel-diode. The effective d-c load is

$$[Z]_{d-c} = \left(R_3 + [Z_{eb}]_{T2} \right) + \left(R_4 + [Z]_{D2} \right) ,$$

which must be kept below the absolute magnitude of the negative resistance of the tunnel-diode. The magnitudes of R_4 and $[Z]_{D2}$, the diode impedance, will be a few ohms each. The value of the negative resistance of a tunnel-diode depends on the peak current. The normal range of the negative resistance values for germanium tunnel-diodes is from five to 250 ohms, corresponding to peak currents of 22 to 0.5 milliamperes.

Equivalent Circuits

Before a rigorous analysis can be made on the relationship between stability and circuit parameters, the equivalent circuits of the active devices, the tunnel-diode and the transistor, have to be examined. Figure 8 shows the equivalent circuit for a tunnel-diode (33). L_s and R_s are the series inductance and resistance respectively; C_d is the capacitance of the junction and g is the differential conductance.

It has been shown that this model is valid for operating frequencies in the GHz (22). The values of the parameters are determined by the quiescent operating point, or the d-c bias voltage for the tunnel-diode. For high frequency microwave tunnel-diodes, L_s, R_s,

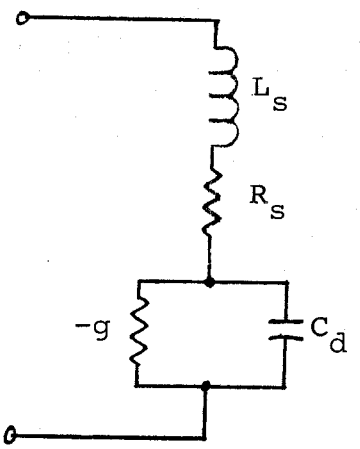

Figure 8. Equivalent circuit of a tunnel-diode.[3]

g and C_d are on the order of 10^{-10} henries, 10^{0} ohms, 10^{-2} mhos and 10^{-13} farads respectively. Direct measurements for these parameters are extremely difficult. Indirect measurements which entail simplifying assumptions are usually employed (1,17). The difficulty in making accurate measurements has an important bearing on the approach of practical circuit design. An elaborate circuit analysis, based on these approximated parameter values, is unwarranted. More emphasis should be placed on the experimental work.

A simplified equivalent circuit for the forward biased emitter-base junction of a transistor is given in

[3] The precise title should have been "The small signal equivalent circuit of a tunnel-diode biased at the negative differential conductance region". Since only the negative differential conductance of the tunnel-diode is of interest here, it is taken for granted that, unless otherwise stated, the tunnel-diode is biased at the negative region. The term g will imply $|-g|$.

Figure 9. This model was chosen because it is simple and more important; also it agrees quite well with experimental results where a fast-risetime current pulse is used for measurement. For high frequency transistors,

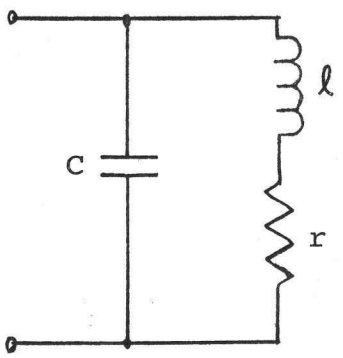

Figure 9. Simplified equivalent circuit for the emitter-base junction of a transistor.

the values of c, ℓ and r are on the order of 10^{-12} farads, 10^{-9} henries and 10^{0} ohms respectively. Again it should be emphasized that the parameter values are a function of the quiescent operating point of the transistor.

The collector junction of a transistor operating at the active region is always reverse biased and therefore represents a large impedance, in the order of 10^{4} ohms or higher. With reference to Figure 7, the collector-base junction impedance of T1 is much larger than that of the tunnel-diode and the emitter-base junction of T2. Consequently the collector junction, in this special case, can be represented by a current source (responsive

to the input signal to T1) shunted by a capacitor, as shown in Figure 10.

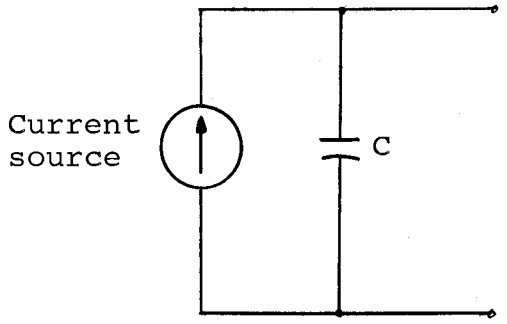

Figure 10. Simplified equivalent circuit for the collector junction of a transistor.

The above presentation is not valid for frequencies higher than a few GHz where the shunting effect of the capacitor C can no longer be neglected.

Stability and Gain of a One-Stage Amplifier

As mentioned previously, the stability of the tunnel-diode circuit depends on the equivalent resistance evaluated in parallel with the tunnel-diode. The problem of stability analysis is reduced to that of finding a suitable equivalent circuit for the amplifier. With reference to Figure 7 on a-c equivalent loading, there are three impedances connected in parallel with the tunnel-diode. R_2 is designed to be quite large compared to $\left(R_3 + \left[Z_{eb}\right]_{T2}\right)$ and can be neglected. Using the results developed in the previous section, the equivalent

circuit for stability analysis will be as shown in Figure 11,

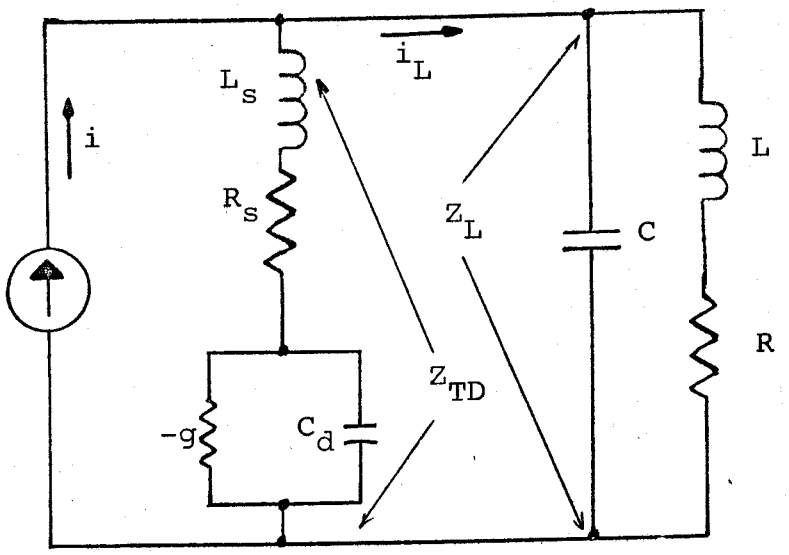

Figure 11. Equivalent circuit for stability and gain analysis.

where L = the inductance due to T2 and the lead inductance,

R = R_3 plus resistance due to T2 (including R_4 and diode resistance also for the d-c load),

C = the sum of the collector junction capacitance due to T1, emitter junction capacitance due to T2 and stray capacitance in the circuit.

The equivalent circuit as shown in Figure 11 is valid only under the following conditions:

(1) The quiescent operating points of T1, T2 and TD are in the linear regions.

(2) T1 and T2 offer effective isolations for the TD from the input source and output load at the operating frequency concerned.

(3) The environmental conditions, such as temperature, are constant.

The expressions for the impedances of the tunnel-diode (9) and its equivalent load in terms of the Laplacian operator "s" will be presented first and then the transfer function between i and i_L, the signal current and the output current respectively will be derived. It is assumed here that the common-base current gain, α, of the transistor is approximately one.

The impedances of the tunnel-diode, Z_{TD}, and its parallel equivalent load, Z_L, are

$$Z_{TD} = \frac{L_s C_d s^2 + (R_s C_d - L_s g)s + (1 - R_s g)}{C_d s - g} ,$$

$$Z_L = \frac{Ls + R}{LCs^2 + CRs + 1} ,$$

where "s" is the Laplacian operator.

The transfer function between i and i_L is

$$\frac{i_L}{i} = \frac{Z_{TD}}{Z_{TD} + Z_L}$$

$$= \frac{a_4 s^4 + a_3 s^3 + a_2 s^2 + a_1 s + a_o}{b_4 s^4 + b_3 s^3 + b_2 s^2 + b_1 s + b_o} , \quad \text{(1)}$$

where

$$a_4 = L_s C_d LC$$

$$a_3 = L_s C_d RC + R_s C_d LC - L_s gLC$$

$$a_2 = L_s C_d + LC - R_s gLC + R_s C_d RC - L_s gRC$$

$$a_1 = RC - R_s gRC + R_s C_d - L_s g$$

$$a_o = 1 - R_s g$$

$$b_4 = a_4$$

$$b_3 = a_3$$

$$b_2 = (L_s C_d + LC - R_s gLC + R_s C_d RC - L_s gRC) + LC_d$$

$$b_1 = (RC - R_s gRC + R_s C_d - L_s g) + C_d R - Lg$$

$$b_o = (1 - R_s g) - Rg.$$

The requirement for stability is that the poles of the transfer function fall in the left half side of the s-plane. This requires that the real parts of the roots of the equation,

$$b_4 s^4 + b_3 s^3 + b_2 s^2 + b_1 s + b_o = 0,$$

be negative (5, p. 469-485). Then, from the Routh-Hurwitz criteria (16, p. 395-422) which gives the requirements for a polynomial to have exclusively negative roots, the necessary and sufficient conditions for stability will be,

$$b_4, b_3, b_2, b_1, b_o > 0,$$

$$\begin{vmatrix} b_1 & b_o \\ b_3 & b_2 \end{vmatrix} > 0,$$

$$\begin{vmatrix} b_1 & b_o & 0 \\ b_3 & b_2 & b_1 \\ 0 & b_4 & b_3 \end{vmatrix} > 0.$$

The stability requirements can be simplified when the following relations, which are generally true in

practice, are taken into consideration,

$$L \gg L_s$$
$$R \gg R_s$$
$$C \approx 10^{-12} \text{ farad.}$$

This being the case, the stability criteria for the amplifier are reduced to the three conditions

$$\frac{1}{g} > R_s + R, \qquad (2)$$

$$R_s > \frac{L_s g}{C_d}, \qquad (3)$$

$$R > \frac{Lg}{C}. \qquad (4)$$

Equation (2) is a mathematical statement of the stability criterion that the negative resistance of the tunnel-diode should be larger than its equivalent load impedance, as mentioned previously. Note that equations (3) and (4) are of the same form, with equation (3) governing the parameters of the tunnel-diode and equation (4) that of the parallel load on the tunnel-diode.

The current gain, given by the transfer function between i_L and i, is accurate for $\omega \leqslant 10^{10} \frac{\text{rad}}{\text{sec}}$. At the higher frequencies, the shunting effect of the capacitor C (which includes the capacitance of the input transistor as well as the stray capacitance of the circuit) will become prominent. Note that the magnitude of C is on the order of 10^{-12} farads. The d-c current gain, A_i, is

$$A_i = \left| \frac{i_L}{i} \right|_{\omega = 0}$$

$$= \frac{1 - R_s g}{1 - R_s g - Rg} \quad . \qquad \text{(5)}$$

From Equation (5), R can be expressed as

$$R = \frac{A_i - R_s g A_i + R_s g - 1}{A_i g} \quad . \qquad \text{(6)}$$

Effects of Temperature and Voltage Supply Variations

Allowable Variation in g

The two most important factors that govern the value of g of a tunnel-diode are the bias voltage and temperature (27). It is evident, from Figure 1, that the differential conductance, g, varies with the bias voltage. Variation in the voltage supply, or having a large input signal voltage, will result in a change of the bias voltage and thus the value of g. The effect of temperature on a tunnel-diode depends on the semiconductor material of which the tunnel-diode is made. Since the basic properties of semiconductor materials are sensitive to temperature, the device's characteristic is expected to be a function of temperature. The manner in which g varies with temperature will be discussed below.

In the previous analysis, in which a constant value of g has been assumed, the amplifier's stability and gain have been shown to be intimately related to the value

of g. The amplifier can tolerate only so much variation in g, due to the various factors just mentioned, and still perform within a specified standard. In view of the more stringent requirements for d-c stability, the d-c gain A_i will be chosen as the standard for comparing the amplifier's performance.

Assuming that ± 30% variations in A_i are allowable, then the corresponding limits for g can be derived from Equation (5). Solving g in terms of A_i, we have

$$g = \frac{A_i - 1}{A_i R_s + A_i R - R_s} \approx \frac{A_i - 1}{A_i R} . \qquad (7)$$

Differentiating Equation (7) with respect to A_i gives,

$$\frac{\triangle g}{\triangle A_i} \approx \frac{1}{A_i^2 R} . \qquad (8)$$

With $\triangle A_i = 0.3\ A_i$, Equation (8) becomes

$$\frac{\triangle g}{g} = (0.3)\ \frac{1}{A_i - 1} . \qquad (9)$$

Equation (9) shows that the higher the gain A_i, the smaller the tolerance is for g. With the allowable variation in A_i being 30%, the allowable percentage variations in g for different values of A_i is shown graphically in Figure 12.

It should be emphasized here that the primary factor determining the range of allowable values of g is the stability requirements stated in Equations (2), (3), and

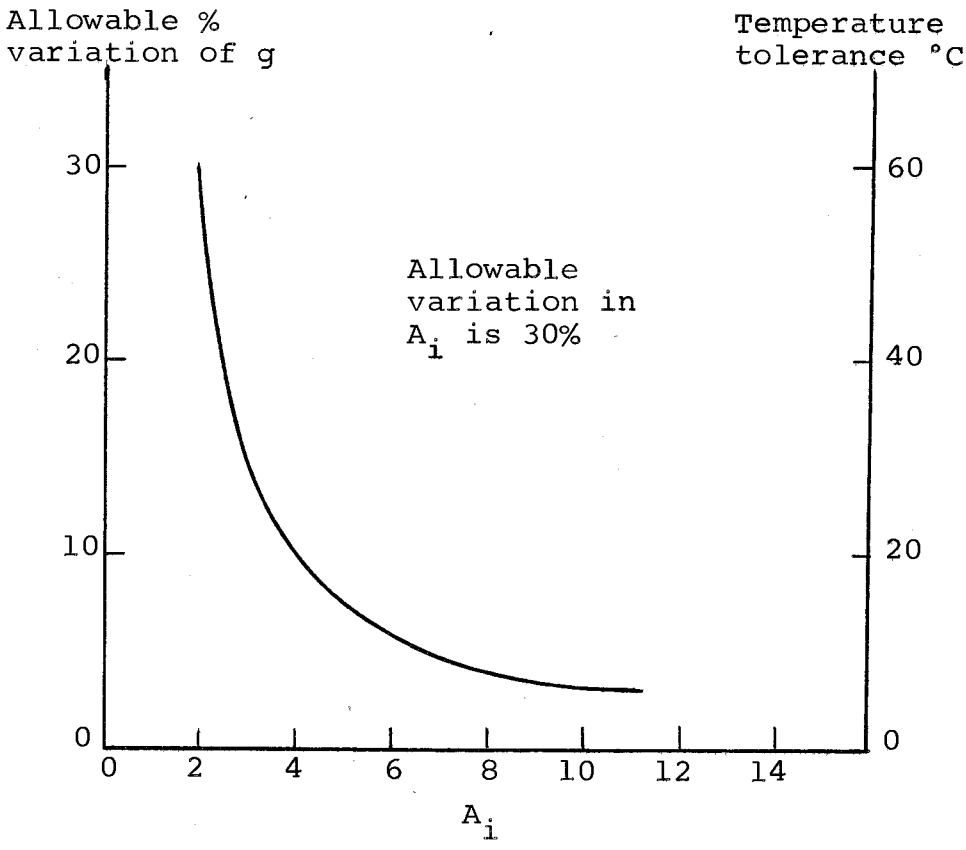

Figure 12. Current gain versus allowable variations in g and temperature.

(4). When a certain range of variations in g is anticipated, the circuit must be designed to allow such variations without violating the stability requirements. In terms of the allowable variations in g, the tolerances on temperature and voltage supply can be defined.

Tolerance on Voltage Supply Variation

Examination of the circuit diagram in Figure 6 shows that both B^+ and B^- voltage supplies affect the

bias voltage and consequently, the value of g of the tunnel-diode. The effect of variation in B^+ will be examined first. The input and output transistors, T1 and T2, are virtually unaffected by small variations in B^+. This is because the voltages at the bases of T1 and T2 are governed by voltage references D1 and ZD. Small changes in collector-base voltage usually do not affect a transistor's performance. However, the tunnel-diode's operating point is definitely modified by the alteration in B^+. Figure 13 shows the relationship between the voltage across the tunnel-diode, which is represented by a negative resistor ($-r_d$), and the B^+.

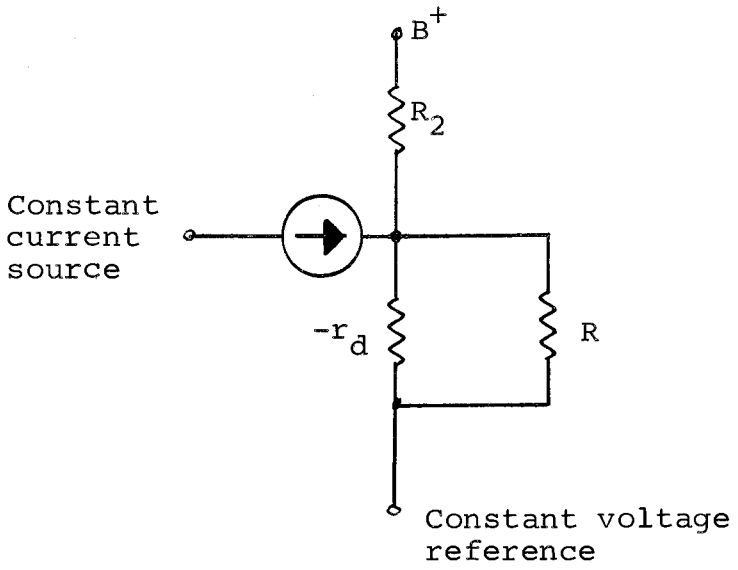

Figure 13. Effect of B^+ on the operating point of the tunnel-diode.

The parallel combination of $(-r_d)$ and R (the load resistance on the tunnel-diode), together with the resistor R_2, form a voltage divider for B^+. The percentage of the change in B^+, $\triangle B^+$, that will appear across the tunnel-diode is,

$$\left(\triangle B^+ \times \frac{\frac{R(-r_d)}{R - r_d}}{R_2} \times 100\% \right) .$$

Specifically for the amplifier to be described, R_2 is designed to be over 5000 ohms. Then, with $|-r_d| = 70$ ohms and R = 50 ohms (corresponding to a d-c gain of three), only 3.5% of $\triangle B^+$ will appear across the tunnel-diode.

It is reasonable to assume that variation in B^+ can be held within 0.1%, in which case only 0.0035% of B^+ will be added to the bias voltage. The normal value of bias voltage for a tunnel-diode is between 70 to 150 millivolts. With the magnitude of 0.0035% of B^+ (19 volts) being well under one millivolt, it is evident that 0.1% variation in B^+ has negligible effect on the tunnel-diode's bias voltage.

The minus voltage supply, B^-, affects only the input transistor T1. With techniques used previously, it can be shown that only 1% of $\triangle B^-$ will appear as input voltage at T1. Comparing to an input voltage level of five millivolts, 0.1% change in B^- will result in a

4% alteration of the input voltage. Again it can be concluded that the probable variation in the minus voltage supply has little effect on the amplifier.

Tolerance on Temperature Variation

The parameter which is most affected by temperature variation in a tunnel-diode is the excess current (6). It always increases with temperature. On the other hand, the peak current I_p can have either a positive or negative temperature coefficient, depending on the type of semiconductor and degree of doping (31). The commercially available germanium tunnel-diodes doped with indium, gallium and arsenic and with a resistivity on the order of 6×10^{-4} ohm-cm have a negative temperature coefficient for I_p. The net result is that the differential conductance g decreases with temperature. The variation in g is quite significant even with a change of ± 30°C in temperature. The temperature coefficient for the differential conductance g of the tunnel-diodes (GE-TD251A) used in the experimental amplifier is estimated (13, p. 12-14) to be -0.5%/°C. In terms of the temperature coefficient the tolerance on temperature variations can be calculated. The result is shown in Figure 12.

Another effect due to the variation in temperature is that V_p and V_o (see Figure 1) tend to shift toward

the origin as temperature increases. The rate of shift for V_o is estimated (13;26, p. 22-27) to be between (0.05) to (0.1) %/°C. If the load line remains constant, the quiescent operating point will move down to a lower current value. This effect can be important when the slopes of the negative resistance and the load line are matched closely, or for the high gain amplifiers. Fortunately, this effect is compensated by the positive temperature coefficient of the ZD, estimated to be 0.04%/°C (23, p. 160). Referring to Figure 6, the bias voltage across the tunnel-diode will decrease when the zener holding voltage increases with temperature. As a result, the load line shifts toward the origin. Since both the load line and the negative portion of the tunnel-diode characteristic curve shift in the same direction with temperature, it tends to stabilize the operating point. Another temperature compensation effect is that the change in voltage drop (due to temperature) across the emitter junction of T2 is offset by that of D2. Similarly, D1 offsets the change in the emitter junction of T1 and thus reduces the temperature fluctuations in the quiescent current of T1.

For an amplifier as a whole, the gain depends not merely on the value of g, but on R, the loading resistance as well. Since R includes two forward biased p-n

junctions, it is temperature sensitive also. The dynamic resistance of a forward biased p-n junction, r_f, can be approximated (14, p. 45-50) as,

$$r_f \text{ (ohm)} = \frac{kT}{q} \frac{1}{I(\text{ma})} , \qquad \text{——————(10)}$$

where k = Boltzmann's constant
q = the charge on an electron
T = the absolute temperature, K
I = forward current in milliampere (ma).

The percentage change of r_f with temperature, evaluated at room temperature T_o = 300°K, can be derived from Equation (10) as,

$$\Delta r_f \Big|_{T_o} = \frac{k}{qI} \Delta T ,$$

or

$$\frac{\Delta r_f}{r_f}\Big|_{T_o} = \frac{\Delta T}{300} . \qquad \text{——————(11)}$$

With Equation (11), r_f is shown to have a temperature coefficient of 0.33%/°C. A 30°C change from room temperature will result in 10% change in r_f. However, the temperature coefficient of R can be considerably less. If r_f is designed to be 20% of R, then R will have a temperature coefficient of only 0.07%/°C. In another case where R is operated as a variable load, as described in the last paragraph on Operation Principles, then its temperature coefficient will approach that of r_f.

Since r_f increases with temperature, it tends to

offset the drop in the amplifier's gain A_i due to the decrease of g with temperature. The calculated temperature tolerances shown in Figure 12 have not included this compensating factor and thus represent the worst cases that can be expected. On the other hand, r_f decreases with reduction in temperature and tends to hold down the increase in gain A_i due to the increase of g (with the reduction in temperature). The characteristic of r_f enhances the thermal stability of the amplifier.

Examples of Practical Design

Even with the simplified amplifier equivalent circuit model, it is difficult to predict the required parameter values for a tunnel-diode to give a specified frequency response. It will be easier to predict the frequency response of an amplifier when a known tunnel-diode is used in the circuit. A certain amount of trial and error is involved in designing an amplifier to a specification. The general procedures in designing the amplifier are:

(1) From the gain requirement, determine the value of R_3 from Equation (6).

(2) Estimate the values of the circuit's and device's parameters experimentally, or from the available specifications.

(3) Check the stability requirements, as stated in Equations (2), (3), and (4).

(4) From Equation (1), calculate the theoretical frequency response of the amplifier.

(5) Repeat the steps with modified circuit parameter values if the desired frequency response has not been obtained.

Five examples of practical amplifier circuits are presented here. They are:

I. One-stage amplifier, conventional circuit

II. One-stage amplifier, thin-film hybrid (TD251A)

III. One-stage amplifier, thin-film hybrid (TD407)

IV. Two-stage amplifier, thin-film hybrid (TD251A)

V. Two-stage amplifier, thin-film hybrid (TD407)

The circuit diagrams of the five amplifiers are given in Figures 14, 15, and 16. The amplifiers were designed around General Electric Company's (GE) TD251A and TD407.

It was evident from the transfer function, Equation (1), that the lower the values of L_s and C_d, the better the frequency response would be for the amplifier. A tunnel-diode with a much higher frequency capability than necessary should be chosen for the circuit.

Table I gives the pertinent data on the major components incorporated in the amplifiers. Based on the components used in the amplifier and the anticipated construction methods to be utilized, the values of the parameters for the equivalent circuit (Figure 11) were estimated[4] to be as shown in Table II.

[4] See Evaluation of Circuit Parameters in Chapter III.

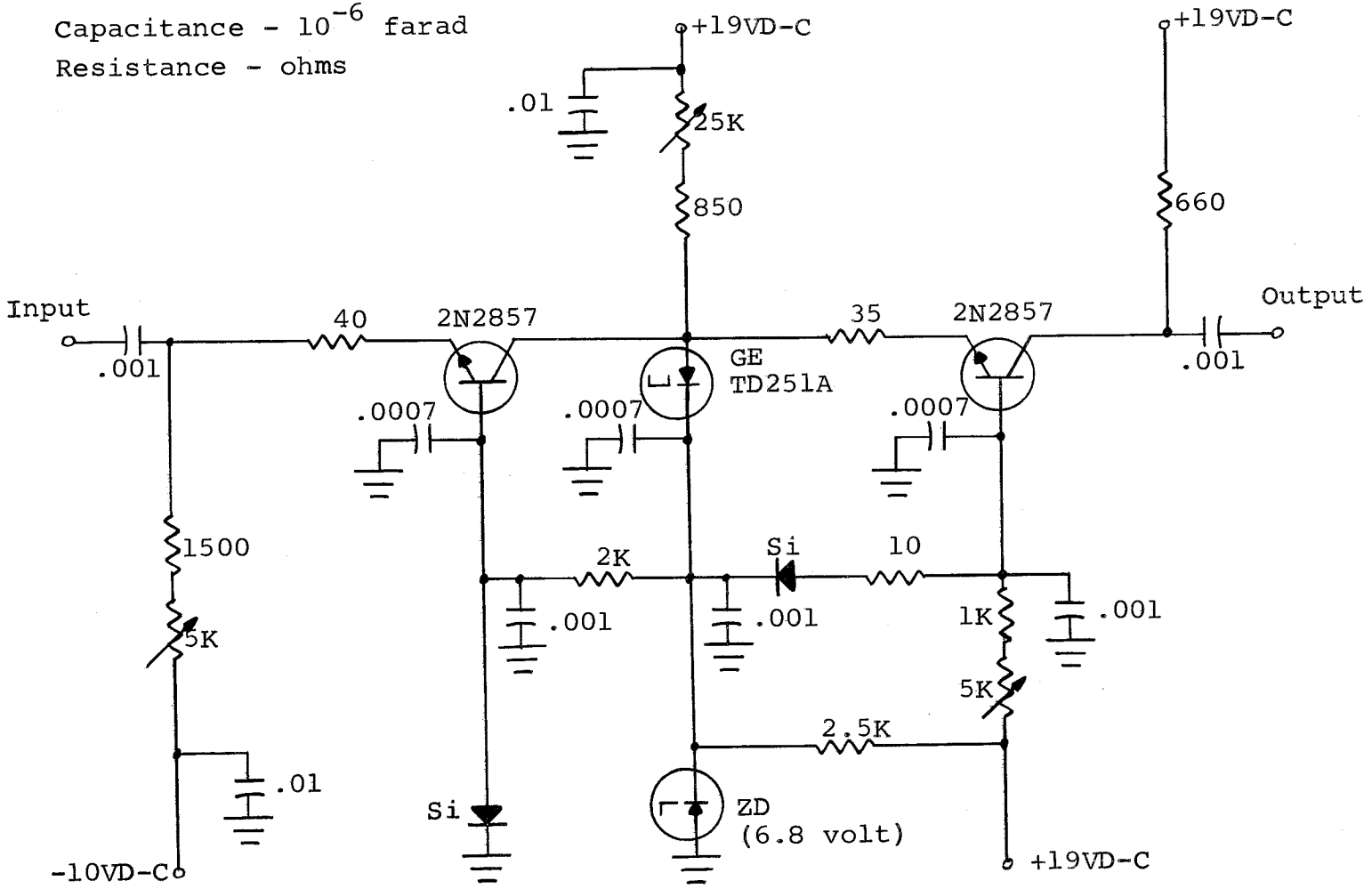

Figure 14. One-stage amplifier, conventional circuit.

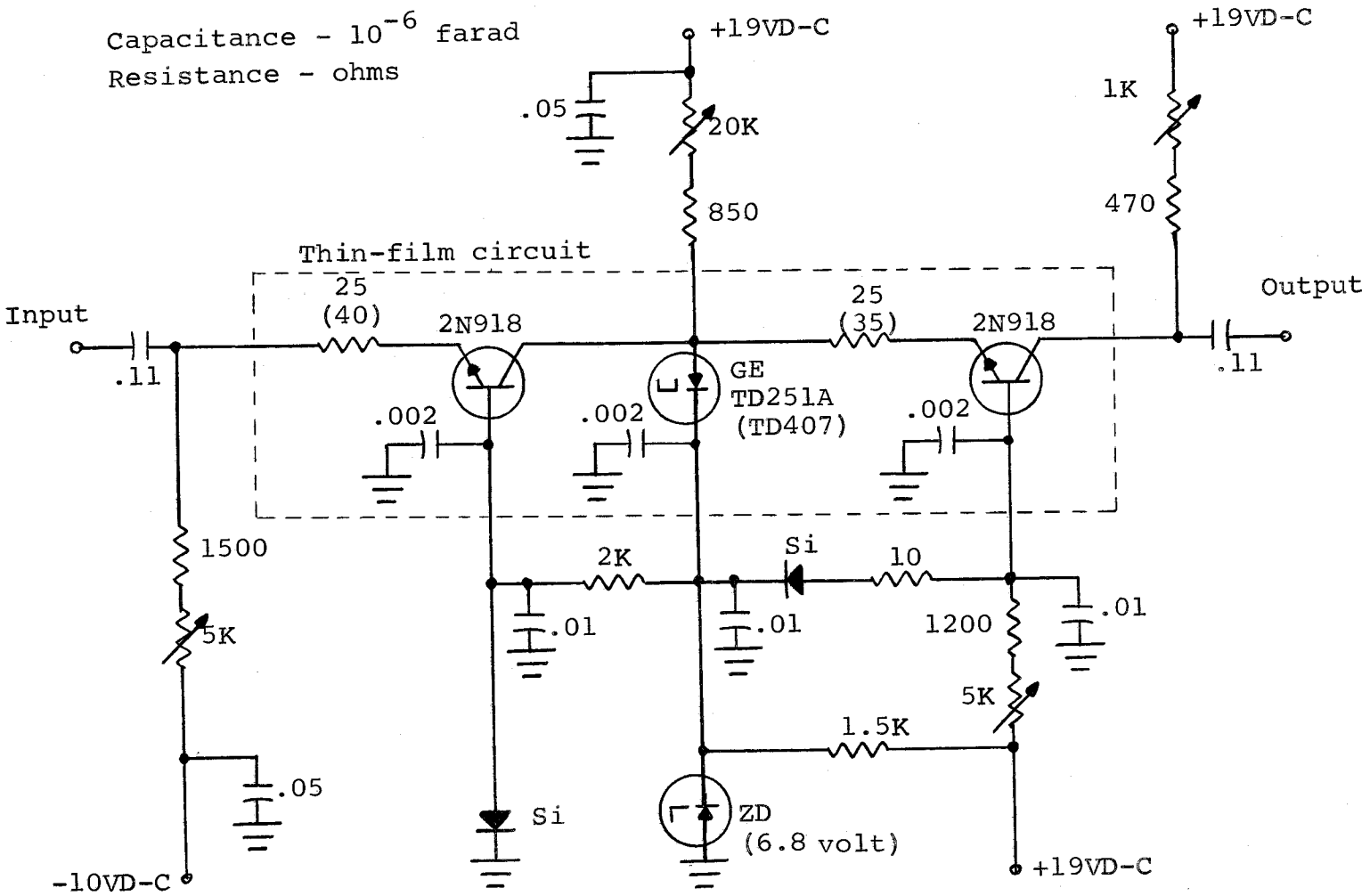

Figure 15. One-stage thin-film amplifiers II and III (in bracket).

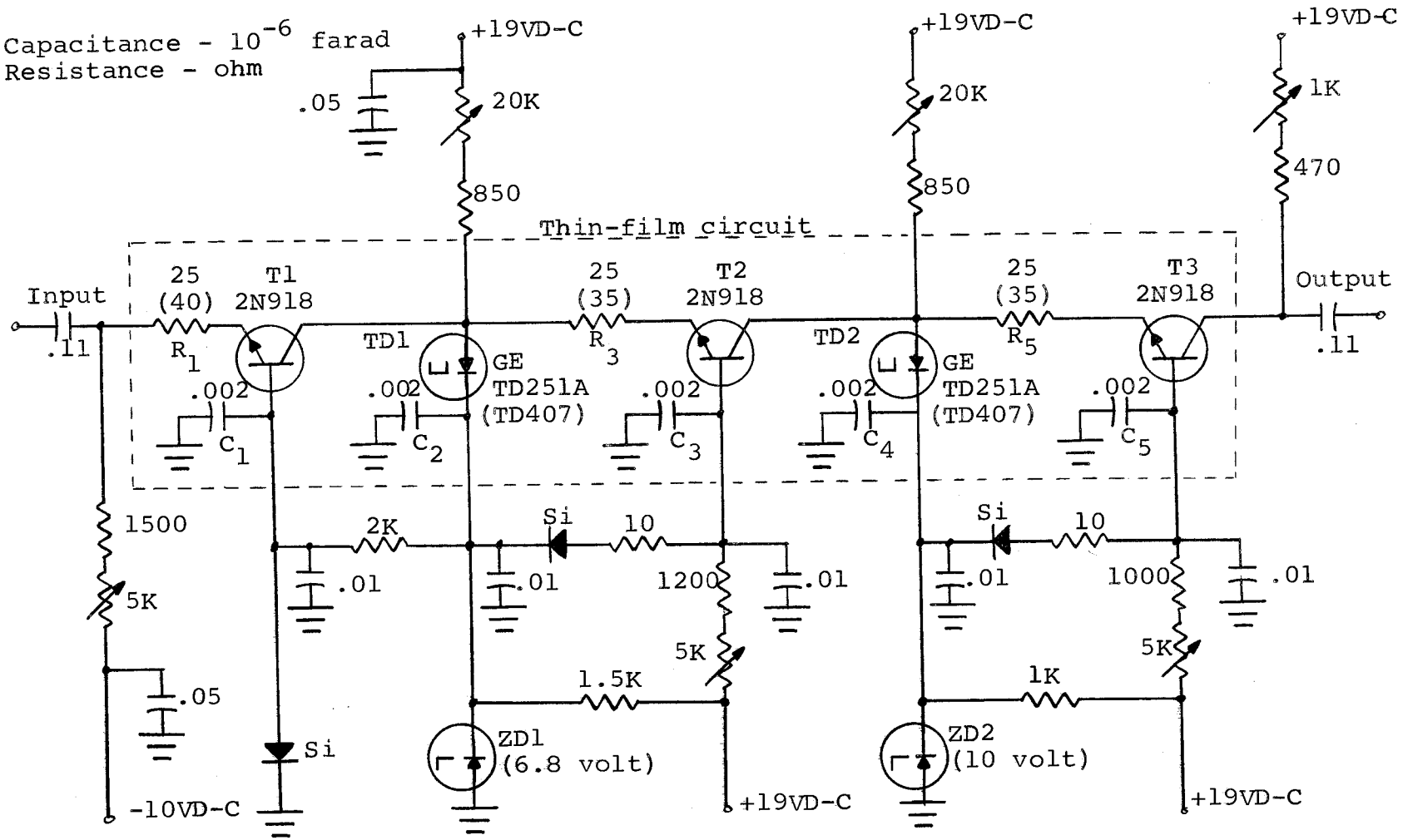

Figure 16. Two-stage thin-film amplifiers IV and V (in bracket).

Table I. Pertinent Data of Transistors and Tunnel-Diodes

	Type	Peak Current I_p (ma)	Peak Point Voltage V_p (mv)	$\lvert -g \rvert$ mho	R_s (ohm)	L_s (10^{-9} henry)	C_d (10^{-12} farad)	Resistive Cutoff freq. f_{ro} (GHz)
Tunnel-Diodes	TD251A (Ge)	2.2±10%	80-90	0.016	7	1.5	1.0	6
	TD407 (Ge)	2.0	80-90	0.014	6	0.1	0.5	35

	Type	Maximum Ratings				Electrical Characteristic		
		Power Dissipation (watt)	V_{CBO} (volt)	V_{EBO} (volt)	I_c (ma)	Output Capacitance (10^{-12} farad)	Input Capacitance (10^{-12} farad)	Gain - Bandwidth Product
Transistors	2N2857 (Si)	0.2	30	2.5	20	1.0	1.5	over one GHz
	2N918 (Si)	0.2	30	3.0	50	1.5	1.5	over one GHz

Table II. Estimated Values of the Amplifier's Equivalent Circuits.

Circuit Construction	Tunnel-Diode					External Load		
	Type	g mho	L_s henry	C_d farad	R_s ohm	L henry	C farad	R ohm
Conventional Circuit	TD 251A	.016	1.5×10^{-9}	3×10^{-12}	7	7×10^{-9}	7×10^{-12}	45
Thin-Film Hybrid	TD 251A	.014	5×10^{-10}	1×10^{-12}	7	5×10^{-9}	3×10^{-12}	35
Thin-Film Hybrid	TD 407	.014	10^{-10}	5×10^{-13}	6	3×10^{-9}	1×10^{-12}	45

The frequency responses of the one-stage amplifiers were calculated from Equation (1). The results are shown in Figure 17. The calculations of the frequency responses of the two-stage amplifiers needed additional justification.

From the study of the effects of temperature and voltage supply variations it was clear that a high gain amplifier should be avoided. To obtain higher gain, the approach of coupling two stages of low gain amplifiers together were tried. The circuit diagram of this two-stage amplifier is shown in Figure 16. Note that the output transistor of stage one becomes the input transistor of stage two. Also, ZD2 has higher holding

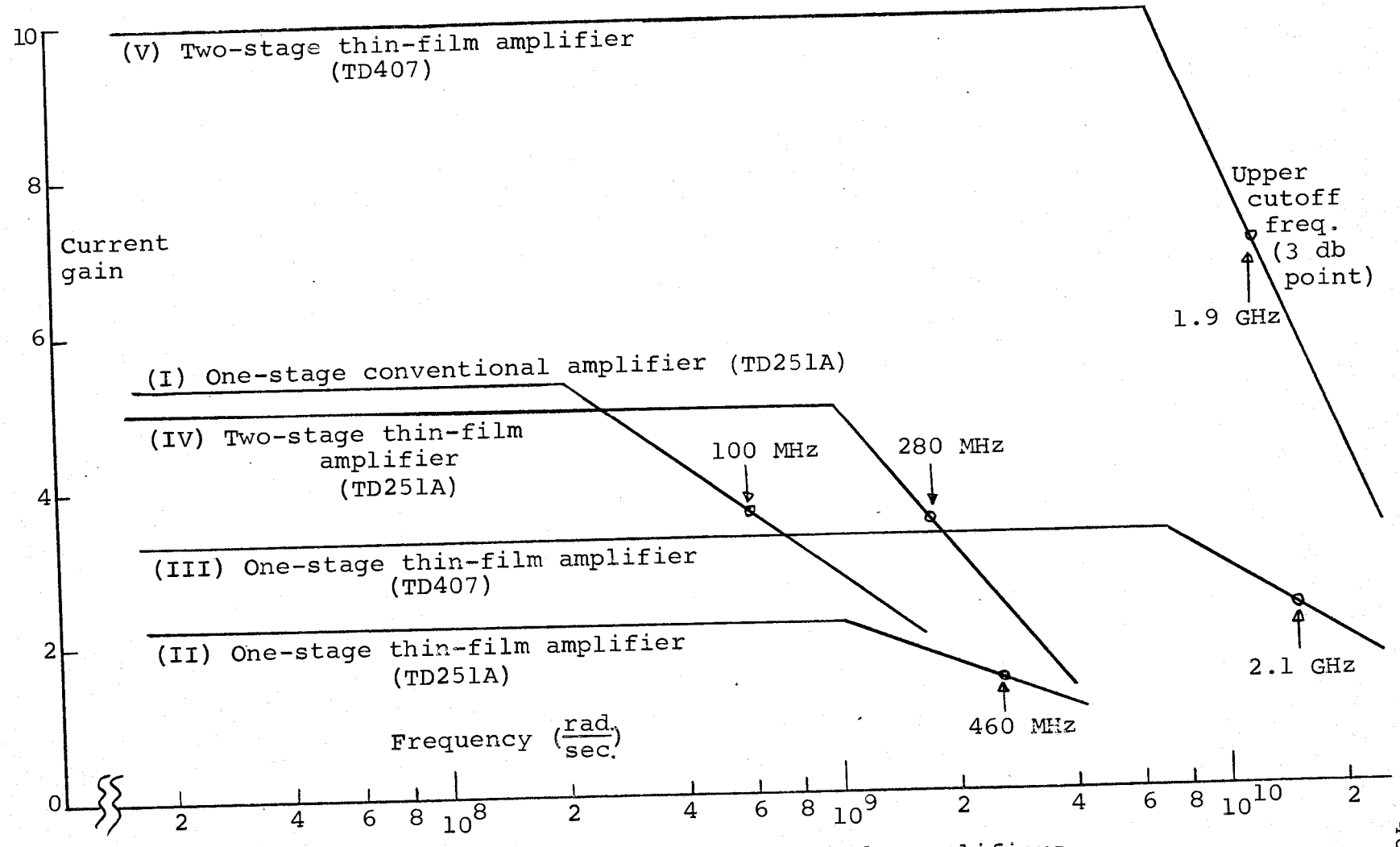

Figure 17. Calculated frequency responses of the amplifiers.

voltage than ZD1 so that T2 will not be operating in the saturation region. With the assumption that T2 offers sufficient isolation between the two stages, the frequency response of this two-stage amplifier can be obtained by squaring the gain of the one-stage amplifier. The calculated frequency responses for amplifiers IV and V are shown in Figure 17.

The conventional amplifier circuit presented here is an example of what can be expected from conventional components. The upper frequency limit is inherently limited to approximately 100 MHz. With thin-film hybrid circuitry, an improvement of five times on the upper frequency limit can be obtained. To extend the upper frequency further into the GHz range requires the stringent optimization of the layout of the thin-film circuit to have minimum distances between the basic elements of the amplifier (see Figure 5) and the use of higher frequency tunnel-diode (TD407).

III. EXPERIMENTAL RESULTS AND CONCLUSION

The Construction of the Amplifiers

Three amplifiers, designed around the TD251A, were constructed. The TD407 tunnel-diode was too expensive ($300/diode) to use in the experimental circuits. Since the aim of the experiments was mainly to prove the feasibility of the design concept, the TD251A will be adequate for that purpose.

Conventional Circuit

Amplifier number I, shown in Figure 14, was constructed with conventional components. Standard soldering techniques were employed. The geometry of the layout was such that the basic elements of the amplifier (see Figure 5) were placed close together. Attempts were made to shorten the lengths of all interconnections to minimize inductance. The final configuration of this conventional circuit is shown in Figure 18.

Thin-Film Hybrid Circuits

As an improvement over the conventional circuit, amplifiers II and IV were made of thin-film circuitry. All the passive elements and their interconnections related to the a-c load (as marked in Figures 15 and 16) were made of thin-film depositions. The active

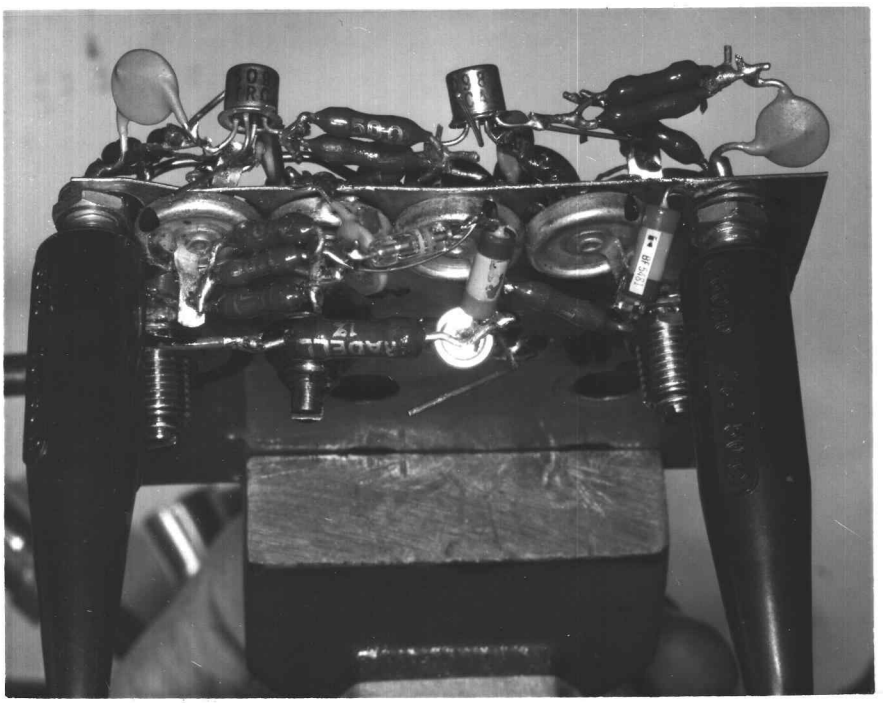

Figure 18. Final configuration of the conventional circuit amplifier.

components, the transistors and tunnel-diodes, were in chip forms and were attached to the thin-film circuit by conducting paint. Data on the construction of this thin-film circuit is in the Appendix.

The main reason in employing thin-film circuitry is to reduce the size of the passive components and the lengths of connections between different components. With the reduction in size and length, the stray capacitances and inductances are greatly reduced. An example of the two-stage thin-film amplifier is shown in Figure 19. The thin-film circuit (as marked by a square) is

seen in the middle of the photograph. A close-up of the thin-film circuit is shown in the Appendix. The conventional components seen in the background are related to the d-c bias circuit.

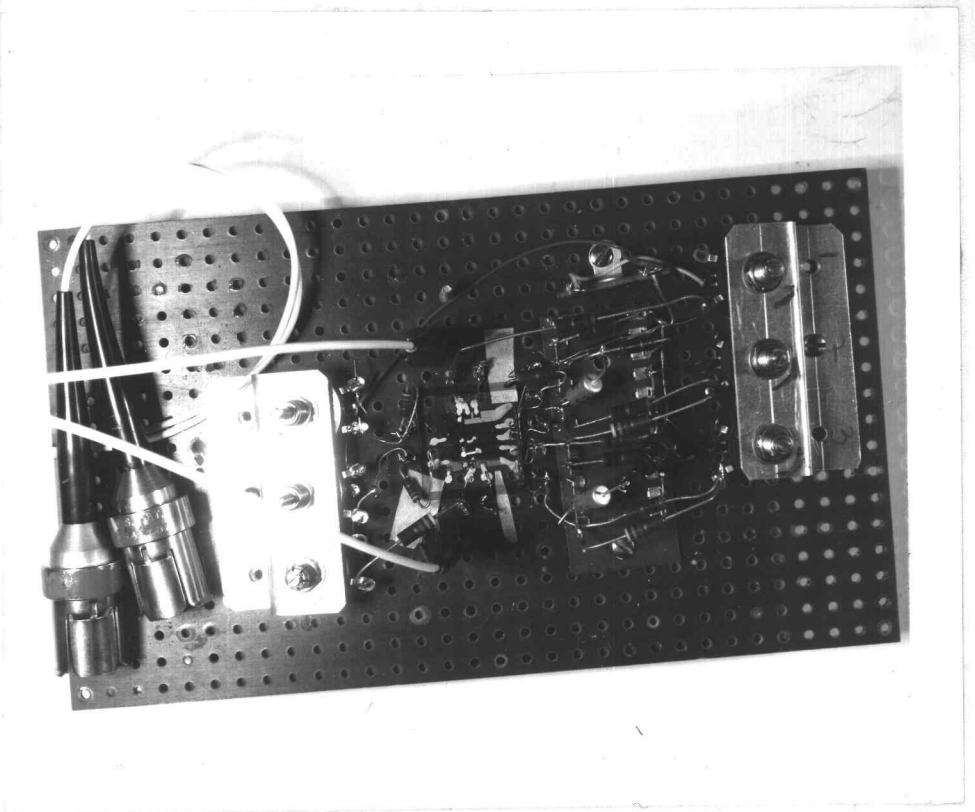

Figure 19. Two-stage thin-film hybrid amplifier.

Estimation of Circuit Parameters

The device specifications furnished valuable information for the estimation of the amplifier's circuit parameters. Some data which were not critical to the amplifier design, or appeared to be reasonable from past experience, were accepted without further experimental measurements. For example, the common-base current gain

of a transistor can be taken to be approximately one (at frequencies below one GHz). Data not available in the specifications were measured experimentally. All components used in the circuit were checked on a curve tracer.

In particular, the peak current and peak voltage of the tunnel-diode were accurately measured. The value of $|-g|$ of the TD251A was modified from the typical value of 0.016 mho (corresponding to a peak current of 2.2 ma) to some lower value when the tunnel-diode had a peak current less than 2.2 ma. The estimated value of the series inductance L_s was much less in the thin-film circuit because the tunnel-diode was in the form of a disk. By comparison with the other packaging specifications for tunnel-diodes, the L_s was estimated to be 0.1 nanohenry (nh) in the thin-film circuit.

Another critical parameter in the amplifier design was the emitter-base impedance of T2, $(Z_{eb})_{T2}$. Since the specifications did not contain information about Z_{eb} for common-base operation, this was determined experimentally. It is known that the input impedance of an emitter-base junction is inherently inductive (14, p. 81-90). The inherent inductance (other than that due to the leads) is caused by the amount of time required for carrier injection and the resulting conductance modulation. The circuit arrangement shown in Figure 20 was used to measure

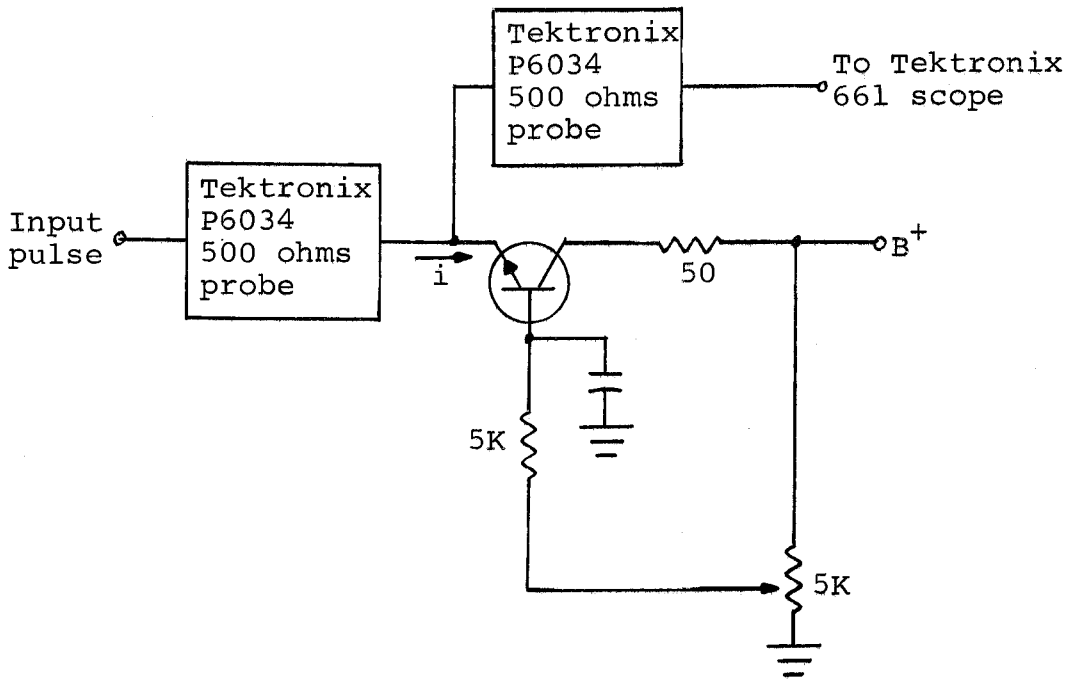

Figure 20. Experimental circuit for measuring the emitter-base impedance.

Z_{eb}. The wave-form of the voltage drop across the emitter-base junction due to a known current-pulse was displayed on an oscilloscope. The voltage drop was composed of $\ell \frac{di}{dt}$ and ri. Knowing the input current pulse, the values of r and ℓ of Z_{eb} can be evaluated. A typical case illustrating this method is shown in Figure 21. With this method, the upper limit of the inductance of Z_{eb} was established as less than ten nanohenries.

The overall inductance L, which includes that of T2, in the equivalent circuit was checked by a resonant-gain experiment. Notice that the tunnel-diode and T2 form a loop circuit that contains R, L and C. Comparing this

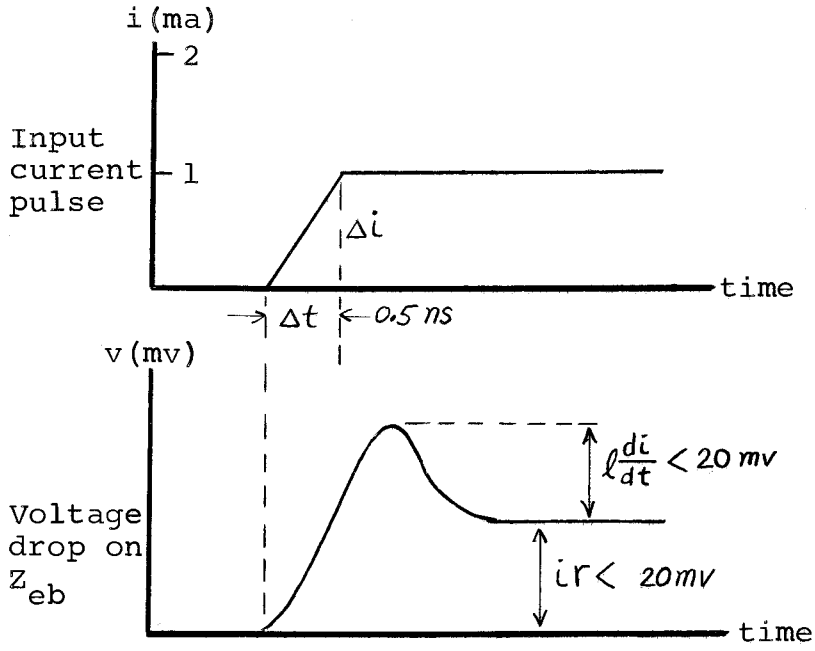

Figure 21. Emitter-base impedance measurement scheme.

combination with a tuned amplifier employing an anti-resonant circuit (8, p. 405-416), the overall inductance L in the equivalent circuit can be recognized as the tuning inductor. The maximum gain of a tuned amplifier occurs at the anti-resonant frequency, f_{ar}, which is given by

$$f_{ar} = \frac{1}{2\pi\sqrt{LC}} . \qquad \text{——————(12)}$$

Equation (12) can be used to give an estimate on the overall inductance L in the equivalent circuit. The gain of the conventional circuit was observed to be peaking at around 600 MHz while that of the thin-film circuit to be at 700 MHz. Assuming that the value of C, the

overall capacitance, was between five to ten picofarads (pf), L was estimated to be around ten nanohenries. This was consistent with the measurement on the inductance of Z_{eb}.

Operation of the Amplifier

Adjustment on the Input Transistor T1

The purpose of the input transistor T1 was to isolate the tunnel-diode from the input source so that it should be operated in the active region at all times. The operating point of T1 was controlled by the adjustment on R_A (see Figure 6). Once the operating point of T1 had been set, then T1 acted as a constant current-sink to the rest of the circuit. Obviously T1 should not be set at a quiescent current higher than the amount that can be furnished through R_2 and T2. Otherwise, the tunnel-diode will be reverse biased and no gain will be available.

Adjustment on the Output Transistor T2

The operating point of the output transistor T2 was the most important factor in the successful operation of the amplifier. It determined the load on the tunnel-diode and also controlled the bias voltage on the tunnel-diode. A detailed description on the biasing of T2 is presented here.

The voltage drop across R_4 and D2 which was controlled by the adjustment of R_D forward biased the output transistor T2. As the forward bias voltage was increased (by decreasing R_D), a point would be reached when T2 can no longer force any more current through T1 (remember that T1 acts as a constant current-sink). Further increase in the forward bias voltage would be counterbalanced by the resulting increase in voltage drop across the tunnel-diode. In this manner the operating point of the tunnel-diode can be varied.

The load on the tunnel-diode also changed as the forward bias voltage was increased. The situation can best be illustrated by graphical method. Figure 22 shows the operating point of the tunnel-diode versus the forward bias voltage. The load lines, which represent the parallel loads on the tunnel-diode at different forward bias voltages, are numbered in order with increasing forward bias voltage. Stability and gain can be obtained only under the condition similar to case 3. The others will result in oscillation or yield a gain less than one. With case 3, there exists a point where maximum gain is obtained. Further increase or decrease in the bias voltage from that point will result in a reduction of gain. All these were observed experimentally.

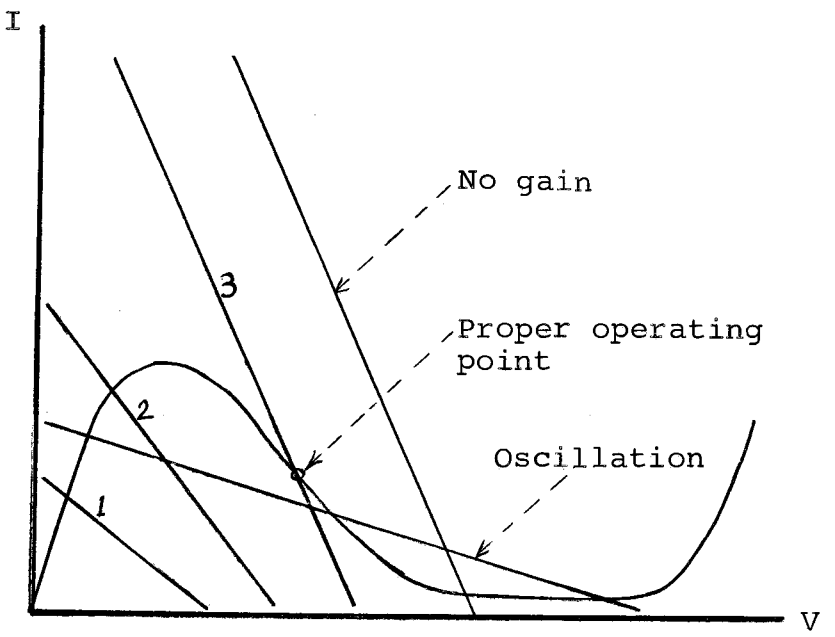

Figure 22. Graphical analysis of the operating point of a tunnel-diode.

Adjustment on R_2

Though the operating point of the tunnel-diode was basically controlled by the bias voltage on T2, minor adjustments, in the form of displacing the load line up and down from the original position, can be made by varying the value of R_2. The voltage drop across R_2 was essentially fixed to be the difference between the B^+ and V_{ZD}, the reference voltage of the ZD. However, the current through R_2 was not constant and it depended on the value of R_2. This is illustrated in Figure 23. The operating point of the tunnel-diode would be shifted

upward or downward in current when R_2 was decreased or increased respectively.

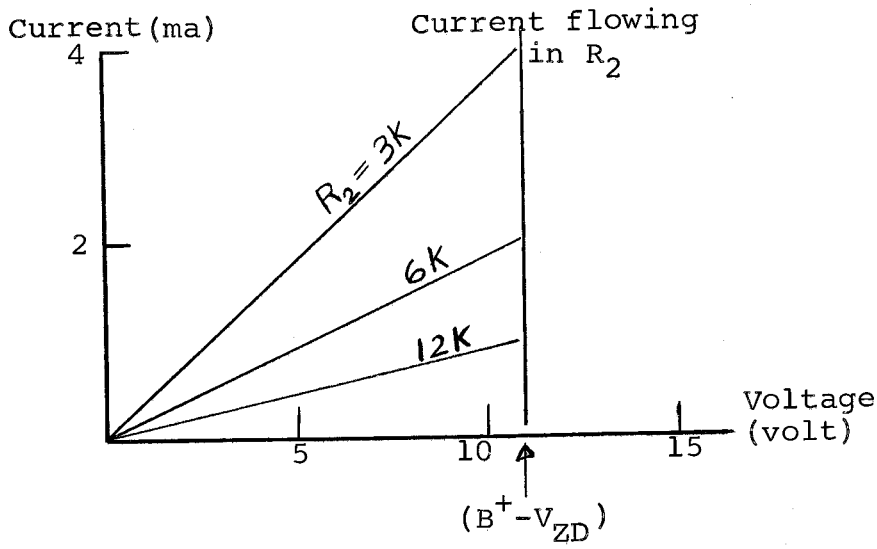

Figure 23. Voltage-current characteristics of R_2.

However, the value of R_2 should not be decreased much beyond ten thousand ohms. That is, the current flowing through R_2 should be limited to approximately one milliampere. The limitation can be visualized from Figure 13. Looking from the collector lead of T1, R_2 is in parallel with the parallel resistance of the tunnel-diode and its load R. Assuming that the negative resistance of the tunnel-diode is 65 ohms and its load resistor R to be 60 ohms, the parallel resistance of this combination will be

$$\frac{(-65)\ (60)}{(-65)\ +\ 60} \approx 800 \text{ ohms.}$$

A considerable portion of the signal current will be lost to R_2 when it is dropped much below ten thousand ohms, and current gain will be reduced. It was observed in the experiment that, when the current in R_2 was increased to approach the limit set by T1, the output transistor T2 was cut off completely, resulting in oscillation or zero output.

Experimental Results and Conclusion

Experimental Results

The tunnel-diode amplifier that has been analyzed, in principle, is capable of having an extremely wide bandwidth, from d-c to the upper cutoff frequency of GHz. It has been the aim of the experiments to show that the design principle is workable and the amplifier is 'practical'. That is, the amplifier can achieve reasonable gain and is stable under normal environmental and electrical disturbances.

The three experimental amplifiers, the conventional circuit and the one- and two-stage thin-film hybrid circuits described in Chapter II, were tested for their frequency responses. Figure 24 shows the block diagram of the testing arrangement.

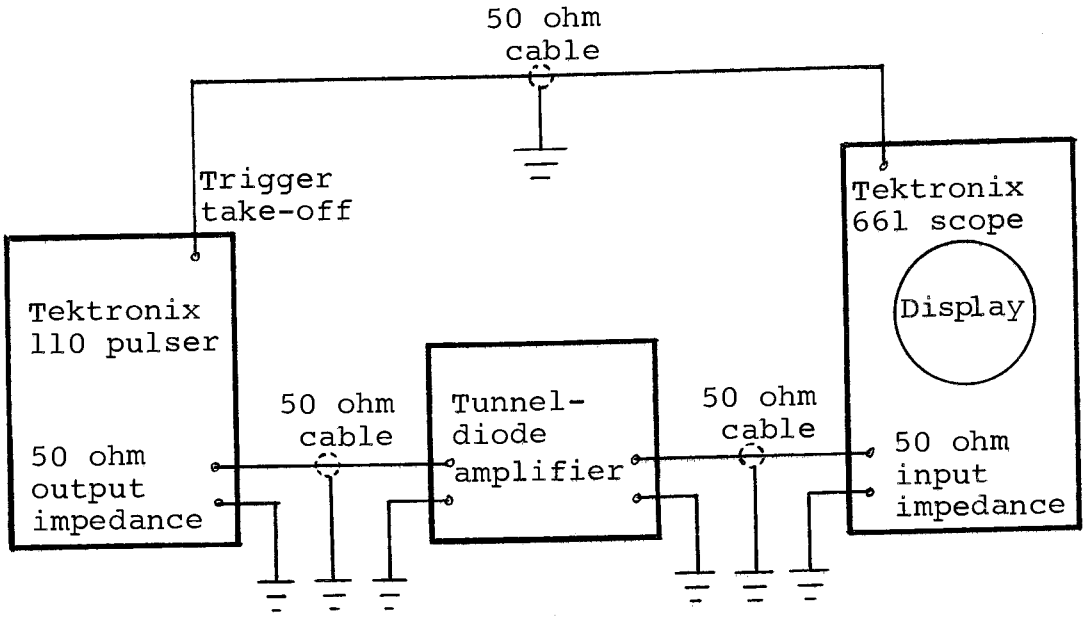

Figure 24. Block diagram for the testing of amplifier frequency response.

The input to the amplifier was a voltage pulse with the following properties (see Figures 25, 26, 28),

magnitude $\approx$ 10 mv
rise time $\approx$ 0.5 nanosecond (ns)
duration $\approx$ 20 or 120 ns .

The output waveform yielded information on the flatness of current gain and the upper cutoff frequency. The fact that 120 ns pulses were amplified (see Figures 25, 28, 29) without much distortion (with the exception of Figure 25) indicated that the amplifiers had constant gains from the upper frequency limits down to frequencies less than one MHz. In the case with the conventional amplifier (Figure 25), the magnitudes of the input and output blocking capacitors were too small to be

effective feedthrough capacitors for the 120 ns pulse. The time constant for the 10^{-9} farad capacitor in series with a few hundred ohms was on the same order of magnitude with the pulse duration. That explained the observed exponential decade in Figure 25. Note that the input and output blocking capacitors, which were responsible for the limitation on the low frequency gain, were introduced only for the convenience of testing.

The upper cutoff frequency of the amplifier was calculated from the rise time of the output pulse. They are related by

$$\underset{(\text{MHz})}{\text{upper cutoff frequency}} \approx 0.35 \frac{1}{\text{rise time (ns)}} .$$

The results obtained with the three amplifiers are summarized in Table III. The theoretical predictions calculated previously are included in the table for comparison. Some discrepancies existed between the predicted and measured values, as shown in Table III. In view of the simplifying assumptions introduced in the formulation of the amplifier's equivalent circuit and the uncertainty involved in determining the parameter values for the tunnel-diodes used, some discrepancies were to be expected and can be tolerated for our purpose.

Table III. Summarized Results on the Frequency Responses of the Experimental Amplifiers.

		Current Gain	Lower Freq. Cutoff (MHz)	Upper Freq. Cutoff (MHz)	Reference	Comment
Conventional Circuit	Predicted	5.5	d-c	100	Fig. 17	Apparently estimated reactance of load impedance was too high, thus a lower frequency limit was predicted
	Measured	5.0	Less than one MHz	145	Fig. 25, 26 and 27	
One-Stage Thin-Film Circuit	Predicted	2.2	d-c	460	Fig. 17	Reasonable agreement
	Measured	2.0	Less than one MHz	440	Fig. 28	
Two-Stage Thin-Film Circuit	Predicted	5.5	d-c	280	Fig. 17	Fig. 30 seems to indicate that oscillations took place at leading edge of output pulse. It could be due to malfunction of scope also.
	Measured	4.0	Less than one MHz	230	Fig. 29 and 30	

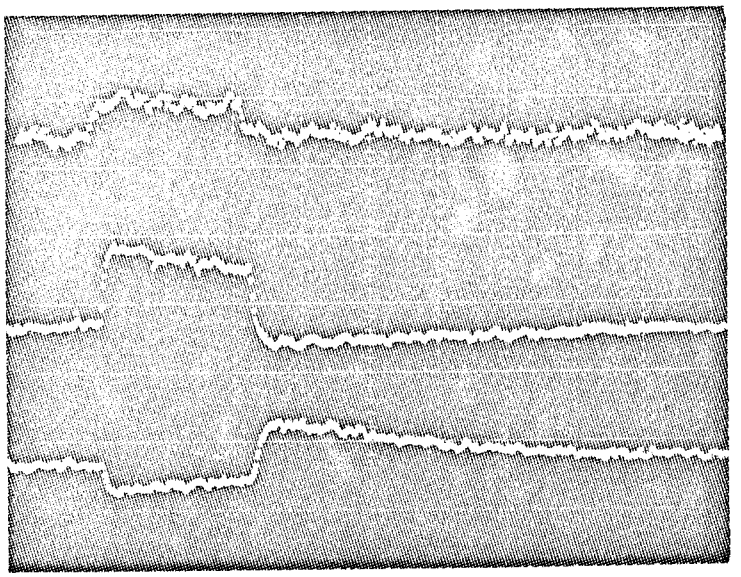

i 50 ns/div. (horizontal) 20 mv/div. (vertical)

ii 50 ns/div. 50 mv/div.

iii 50 ns/div. 50 mv/div.

Figure 25. Output responses with "+" and "-" input pulses of 120 ns duration, Amplifier I.

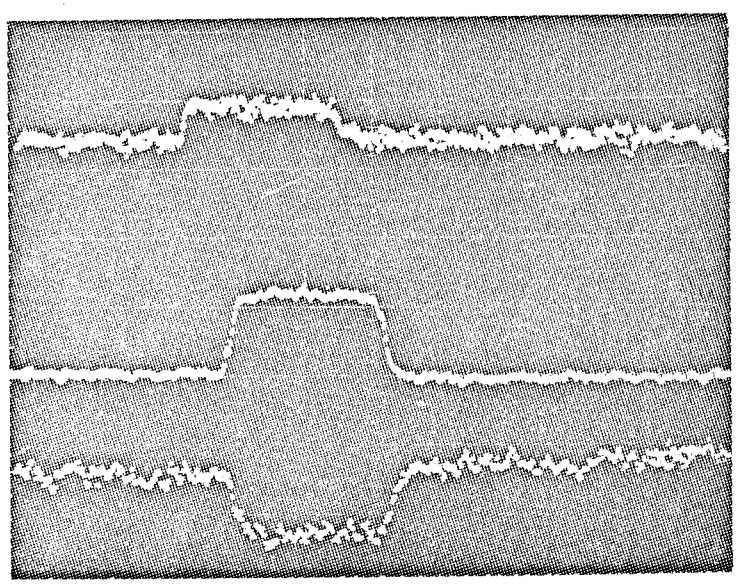

i 10 ns/div. 20 mv/div.

ii 10 ns/div. 50 mv/div.

iii 10 ns/div. 20 mv/div.

Figure 26. Output responses with "+" and "-" input pulses of 20 ns duration, Amplifier I.

	i	ii	iii
Fig. 25	Input pulse	Output pulse	Output pulse with "-" input
Fig. 26	Input pulse	Output pulse	Output pulse with "-" input

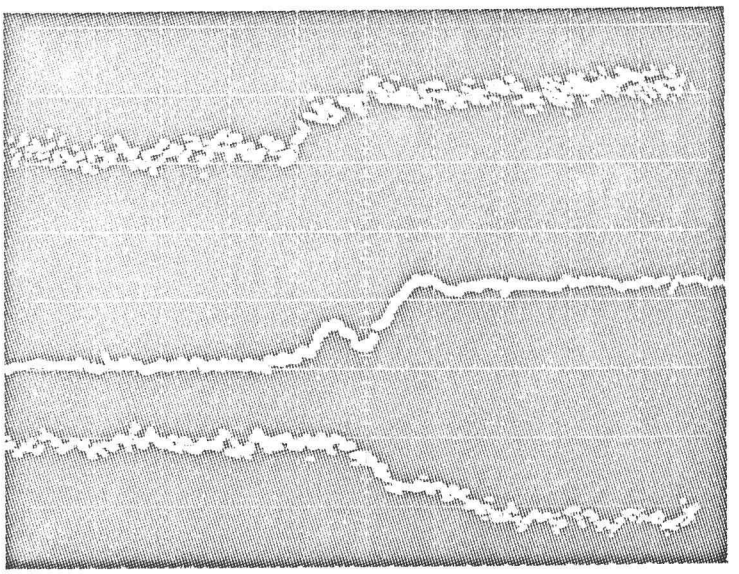

i 1 ns/div. (horizontal) 10 mv/div. (vertical)

ii 1 ns/div. 50 mv/div.

iii 1 ns/div. 20 mv/div.

Figure 27. Risetimes of input and output, Amplifier I.

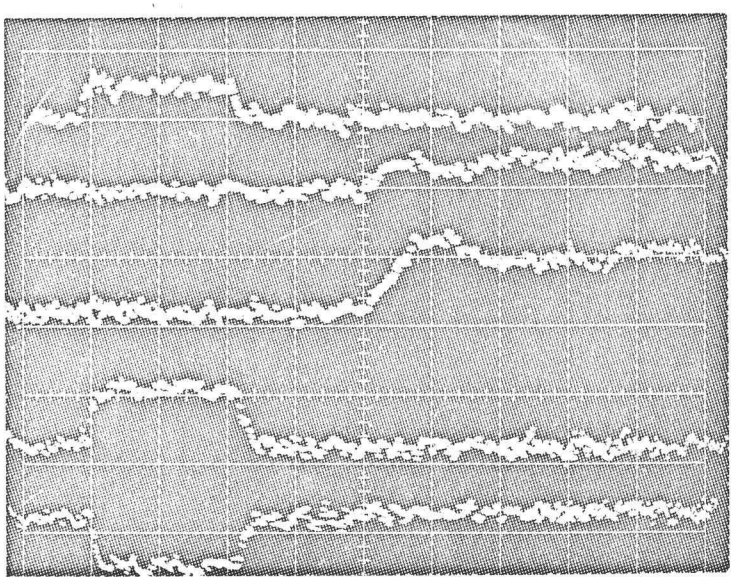

i 50 ns/div. 20 mv/div.

ii 1 ns/div. 20 mv/div.

iii 1 ns/div. 20 mv/div.

iv 50 ns/div. 20 mv/div.

v 50 ns/div. 20 mv/div.

Figure 28. Frequency response of Amplifier II.

	i	ii	iii	iv	v
Fig. 27	Risetime, input pulse	Risetime, output pulse	Risetime, output, with "-" input		
Fig. 28	Input pulse	Risetime, input pulse	Risetime, output pulse	Output pulse	Output pulse, with "-" input

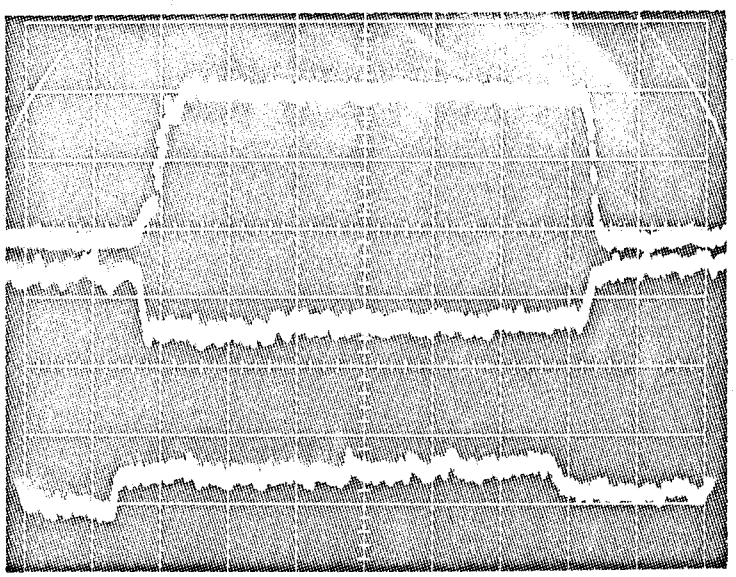

i 20 ns/div. (horizontal) 20 mv/div. (vertical)

ii 20 ns/div. 10 mv/div.

iii 20 ns/div. 10 mv/div.

Figure 29. Output responses with "+" and "-" input pulses of 120 ns duration, Amplifier IV.

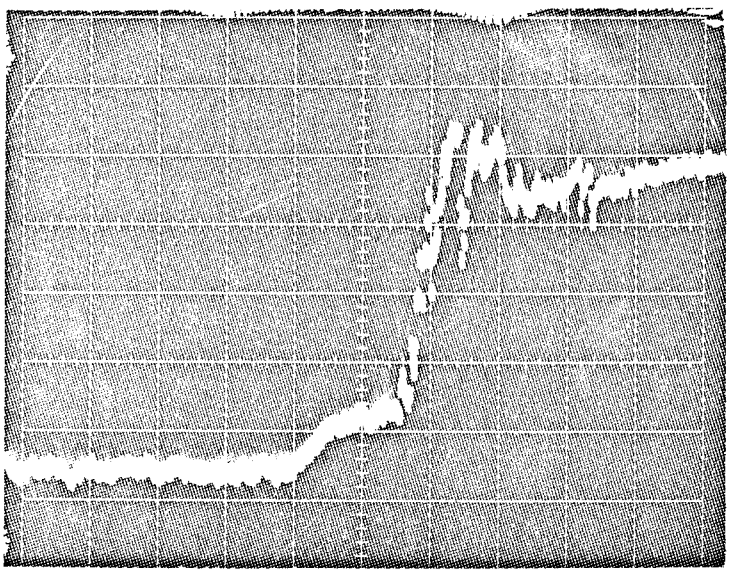

1 ns/div.
10 mv/div.

Figure 30. Risetime of Amplifier IV.

	i	ii	iii
Fig. 29	Output pulse	Output pulse, with "-" input	Input pulse
Fig. 30	Risetime, output pulse		

The operating point of the tunnel-diode was approximated by d-c measurements. The approximation was complemented by a dynamic measurement. By comparing the gains obtained with a positive and a negative input pulse (of the same amplitude), the operating point of the tunnel-diode was deduced. Figure 31 shows three possible operating points of the tunnel-diode. When the gains were the same for both pulses, as was the case shown in Figure 32, the tunnel-diode's operating point must be close to point B of Figure 31. When unsymmetrical gains were obtained, the operating point of the tunnel-diode would be at either A or C, corresponding to the cases shown in Figures 33 and 26.

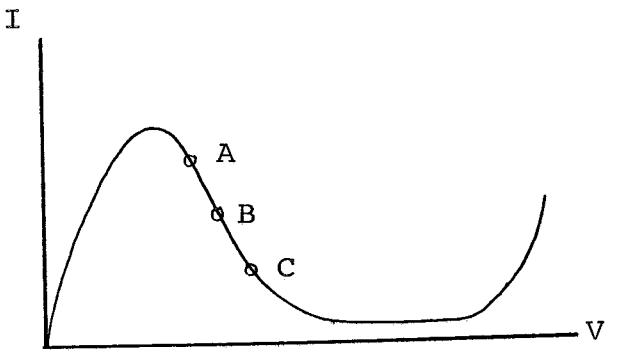

Figure 31. Possible operating points of tunnel-diode.

Adjustment of the operating point was relatively simple for the one-stage amplifier. However, similar attempts on the two-stage amplifier failed consistently. The problem was that the operating points of each of the

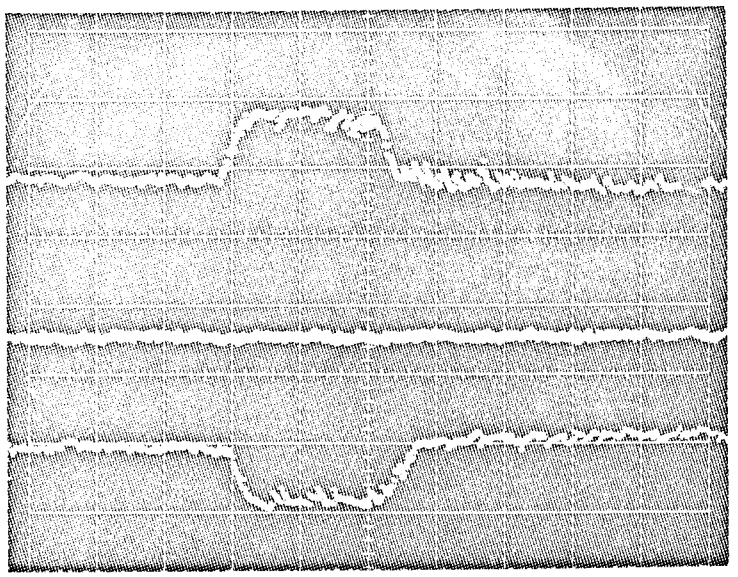

i 10 ns/div. (horizontal) 50 mv/div. (vertical)

ii 10 ns/div. 50 mv/div.

iii 10 ns/div. 50 mv/div.

Figure 32. Symmetrical gains with "+" and "-" inputs, Amplifier I.

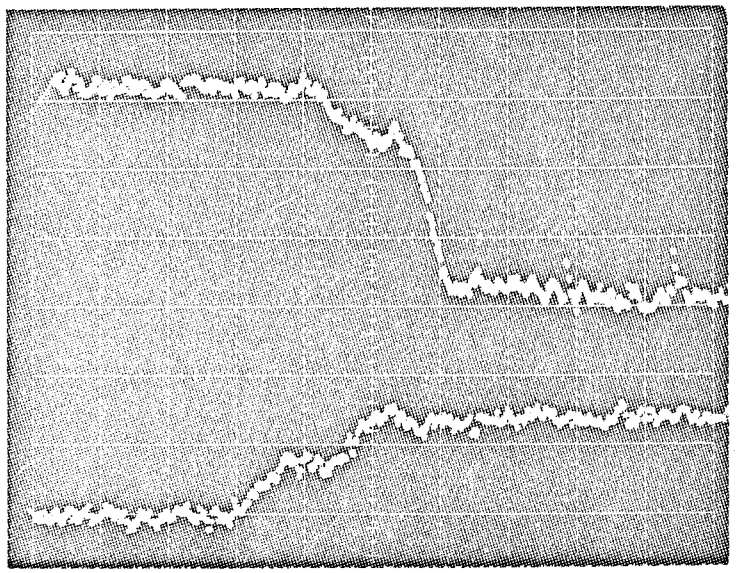

i 1 ns/div. 20 mv/div.

ii 1 ns/div. 20 mv/div.

Figure 33. Risetimes with "+" and "-" input pulses, Amplifier I.

	i	ii	iii
Fig. 32	Output pulse	Output, with no input	Output pulse with "-" input
Fig. 33	Risetime, output with "-" input	Risetime, output	

two tunnel-diodes could not be determined by d-c measurement alone; the anodes of the two tunnel-diodes were not accessible for direct voltage measurement. The a-c measurements of the operating points were complicated by the fact that the output depended on both operating points and adjustments on one operating point might affect the other. A certain amount of coupling between the stages was suspected. An improved design which will allow more independent adjustment on each stage and direct access for measuring the operating point of each tunnel-diode will be needed for the successful operation of the two-stage amplifier.

The other pertinent results which are related to practical applications of the amplifier will be presented to complete the investigation. The effect of temperature variation on gain was examined and the result was consistent with the theoretical analysis. Figure 34 shows the gain variations under different temperature environments. At 20°C above room temperature the steady state gain was reduced by approximately 20%, which was within the limits predicted.

An investigation on the effect of voltage supply variation was carried out also. Noticeable changes in gains were observed when variations of ± 150 mv from the B^+ = 19 volts, or ± 100 mv from B^- =-10 volts were

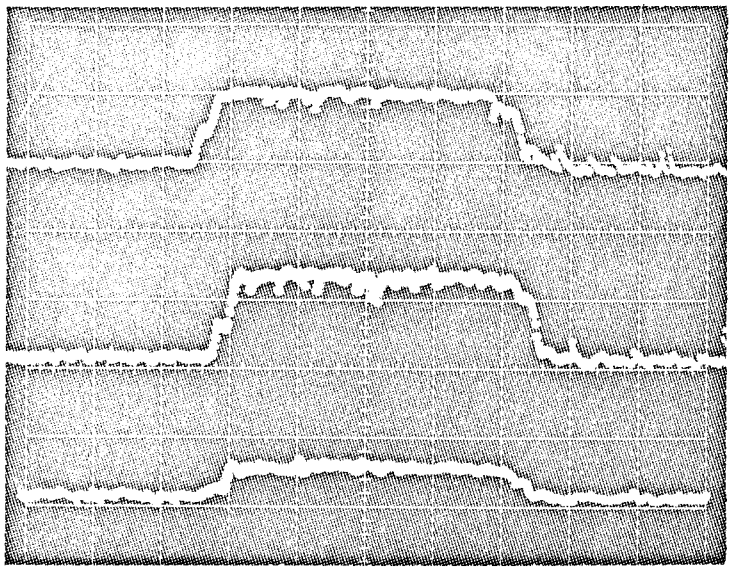

i 5 ns/div. (horizontal) 50 mv/div. (vertical)

ii same

iii same

Figure 34. Variation of gain with temperature, Amplifier I.

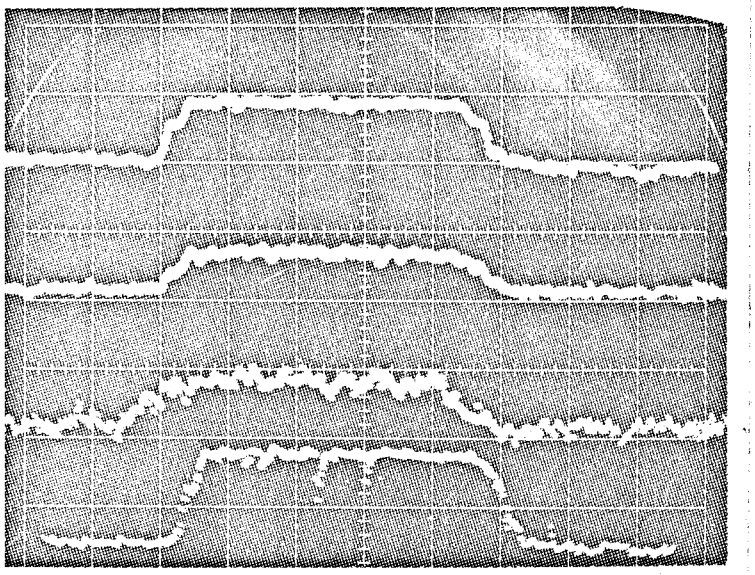

i 5 ns/div. 50 mv/div.

ii 5 ns/div. 50 mv/div.

iii 5 ns/div. 20 mv/div.

iv 5 ns/div. 50 mv/div.

Figure 35. Variation of gain with input magnitude, Amplifier I.

	i	ii	iii	iv
Fig. 34	Output pulse, T = 42°C	Output pulse, T = 23°C	Output pulse, sudden change in T	
Fig. 35	Output pulse, input=10mv	Output pulse, input=5mv	Output pulse, input=2.5mv	Output pulse, input=15mv

introduced. The variations were approximately 1% of the B^+ and B^- and were ten times that to be expected from a regulated voltage supply.

Throughout the theoretical analysis, the non-linearity of the tunnel-diode characteristic was stressed. The equivalent circuit analysis was carried out on the assumption that the a-c signal would be small. A large signal would displace the position of the operating point and the current gain would be affected. This non-linearity in gain for large a-c signal was observed in the experiment. Figure 35 shows the output waveforms for inputs with magnitudes varying from 2½ to 15 mv. The gains changed, approximately, from seven to four as the inputs were increased. This will be a limitation on the application of the tunnel-diode amplifier.

Summary and Conclusion

Wideband tunnel-diode amplifiers using common-base transistor stages for isolation were investigated theoretically and experimentally for stability, frequency response, and the effects of temperature and voltage supply fluctuations. The theoretical analysis determined the current transfer function which predicts the frequency response of the amplifier, and three stability requirements. The analysis also showed that the tolerance on variations in temperature and voltage are

inversely proportional to the gain of the amplifier.

Three amplifiers, a one-stage conventional circuit, and one- and two-stage thin-film circuits were constructed and tested for their frequency responses. The results are shown in Table III. Effects of temperature and voltage supply variations were found to be within the theoretical predictions.

The above results represent a workable model of tunnel-diode amplifier capable of having a constant gain over a frequency spectrum from d-c to 500 MHz. The design of this amplifier, which calls for isolation of the tunnel-diode from the input and output loads and so provides a relatively constant load on the tunnel-diode over the desired frequency spectrum, does not limit itself to the present frequency spectrum. The same principle can be applied to extend the upper frequency limit to approximately two GHz when higher frequency tunnel-diodes and better circuit construction techniques are employed.

BIBLIOGRAPHY

1. Bonin, E. L. and J. R. Biard. Tunnel-diode series resistance. Proceedings of the Institute of Radio Engineers 49 (11):1679. 1961.

2. Boyet, H., D. Fleri and R. M. Kurzrok. Broadband hybrid-coupled tunnel-diode amplifier in the UHF region. Proceedings of the Institute of Electrical and Electronics Engineers 50(6):1527. 1962.

3. Boyet, H., D. Fleri and C. A. Renton. Stability criteria for a tunnel-diode amplifier. Proceedings of the Institute of Radio Engineers 49:1937. 1961.

4. Chen, C. H. Tunnel-diode amplifier. Semiconductor Products 5(4):19-25. 1962.

5. Chen, W. H. The analysis of linear systems. New York, McGraw-Hill, 1963. 577 p.

6. Chynoweth, A. G., W. L. Feldman and R. A. Logan. Excess tunnel current in Si Esaki junctions. Physical Review 121:684. 1961.

7. Clorfeine, A. S. Unconditional stability in tunnel-diode amplifiers. RCA Review 24(1):94-104. 1963.

8. Cutler, Phillip. Semiconductor circuit analysis. New York, McGraw-Hill, 1964. 642 p.

9. Davidsohn, U. S., Y. C. Hwang and G. B. Ober. Designing with tunnel-diode, Part 1 and 2. Electronic Design 8(3):50-58 and 8(4):66-73. February 1960.

10. Davidson, L. A. Optimum stability criterion for tunnel-diodes shunted by resistance and capacitance. Proceedings of Institute of Electrical and Electronics Engineers 51:1233. 1963.

11. Esaki, L. New phenomenon in narrow germanium p-n junctions. Physical Review 109:603. 1958.

12. Frisch, I. T. A stability criterion for tunnel-diodes. Proceedings of the Institute of Electrical and Electronics Engineers 52:922-923. 1964.

13. General Electric Company. Tunnel-diode manual, 1st ed. New York, General Electric Company, 1961. 96 p.

14. Gray, P. E. et al. Physical electronics and circuit models of transistors. New York, John Wiley & Sons, 1964. 262 p. (Semiconductor Electronics Education Committee, Vol. 2)

15. Gruenberg, H. A normalized stability plot for tunnel-diode circuits. Proceedings of the Institute of Electrical and Electronics Engineers 52:773. 1964.

16. Guillemin, E. A. The mathematics of circuit analysis. New York, John Wiley & Sons, 1949. 590 p.

17. Hauer, W. B. Definition and determination of the series inductance of tunnel-diodes. Transactions of the Institute of the Radio Engineers ED-8 (6):470-475. 1961.

18. Hines, M. E. High-frequency negative-resistance circuit principles for Esaki diode applications. Bell System Technical Journal 39:477-513. 1960.

19. Jonscher, A. K. The physics of the tunnel-diode. British Journal of Applied Physics 12:654-659. 1961.

20. Lepoff, J. H. and G. J. Wheeler. Octave bandwidth tunnel-diode amplifier. Transactions of the Electrical and Electronics Engineers MIT-12(1):21-25. 1964.

21. Long, E. D. and C. P. Wowack. Designing tunnel-diode R-F amplifier. Electronics 34(7):120. 1961.

22. McPhun, M. K. The equivalent circuit of the tunnel-diode. Proceedings of the Institute of Electrical and Electronics Engineers 52(12):1754. 1964.

23. Motorola, Inc. Silicon zener diode and rectifier handbook. Phoenix, Motorola Semiconductor Products Division, 1961. 184 p.

24. Neoson, B. W. and R. Masens. Stability criteria for tunnel-diode circuits. Electro-Technology 73(6):52-58. 1964.

25. Pucel, R. A. Physical principles of the Esaki diode and some of its properties as a circuit element. Solid State Electronics 1:22. 1960.

26. Radio Corporation of America. Tunnel diodes. New York, RCA Semiconductor and Materials Division, 1963. 159 p.

27. Schaffner, G. A compact tunnel-diode amplifier for ultrahigh frequencies. Institute of Radio Engineers, Wescon Convention Record 1960, Part 2, p. 86-93.

28. Seitzer, D. A diagram for stability, gain and bandwidth of a linear one-stage tunnel-diode amplifier. Proceedings of the Institute of Electrical and Electronics Engineers 51:1157. 1963.

29. Sie, John J. Absolutely stable hybrid coupled tunnel-diode amplifier. Proceedings of the Institute of Radio Engineers 48:1321. 1960.

30. Simonov, Yu. L. Application of tunnel-diodes in tuned transistor amplifiers. Telecommunications and Radio Engineering Part I, 18(6):40-47. June 1964. (Translated from Elektrosvyaz, USSR)

31. Singh, H. Circuit principles and applications of tunnel-diodes. Control 7:290-294. Dec. 1963.

32. Smilen, L. I. and D. Youla. Stability criteria for tunnel-diodes. Proceedings of the Institute of Radio Engineers 49:1206-1207. 1961.

33. Sommers, H. S. Tunnel-diodes as high-frequency devices. Proceedings of the Institute of Radio Engineers 47:1201. 1959.

34. Steinhoff, R. and F. Sterzer. Microwave tunnel-diode amplifiers with large dynamic range. RCA Review 25(1):54-66. 1964.

APPENDIX

CONSTRUCTION OF THE THIN-FILM CIRCUIT

The base material of the thin-film circuit was a one-inch by three-inch microscope slide. Before the deposition, the slide was cleaned ultrasonically in a detergent solution. Precautions were taken to minimize contamination due to handling and dust in the air. After the slide was put into the evacuation chamber and the pressure pumped down, glow discharge was introduced to further clean the surface of the slide. A controlled amount of argon gas was fed into the evacuated chamber. At the same time, a high voltage (approximately 600 volt a-c) was applied between the metal base of the chamber and an insulated post in the chamber. A glow discharge was obtained when enough argon gas was present to increase the pressure (from 0.1 micron) to 50 microns. The quality of the film depended greatly on the cleanliness of the slide's surface.

The masks for the depositions were made of stainless steel sheets of 0.001 inch thick. The etched patterns of the four masks used for the circuit are shown in Figure 36. The vacuum chamber layout for the thin-film evaporations, as shown in Figure 37, shows the geometric relationship between the source of evaporant and the symmetrically placed thin-film circuit board and the monitoring plate. Some electrical contacts and

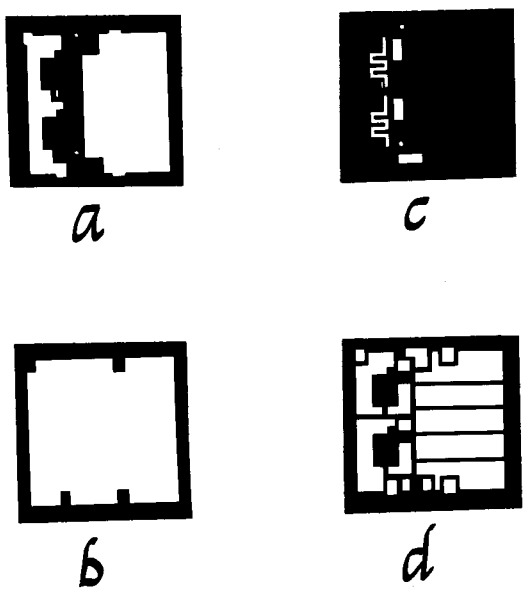

Figure 36. Masks used for thin-film depositions.

a. First mask used; Al evaporation, depositing the ground plane.

b. Second mask used; SiO evaporation, depositing the insulation layer.

c. Third mask used; Nichrome evaporation, depositing the resistors.

d. Last mask used; Al evaporation, depositing the interconnections and capacitors.

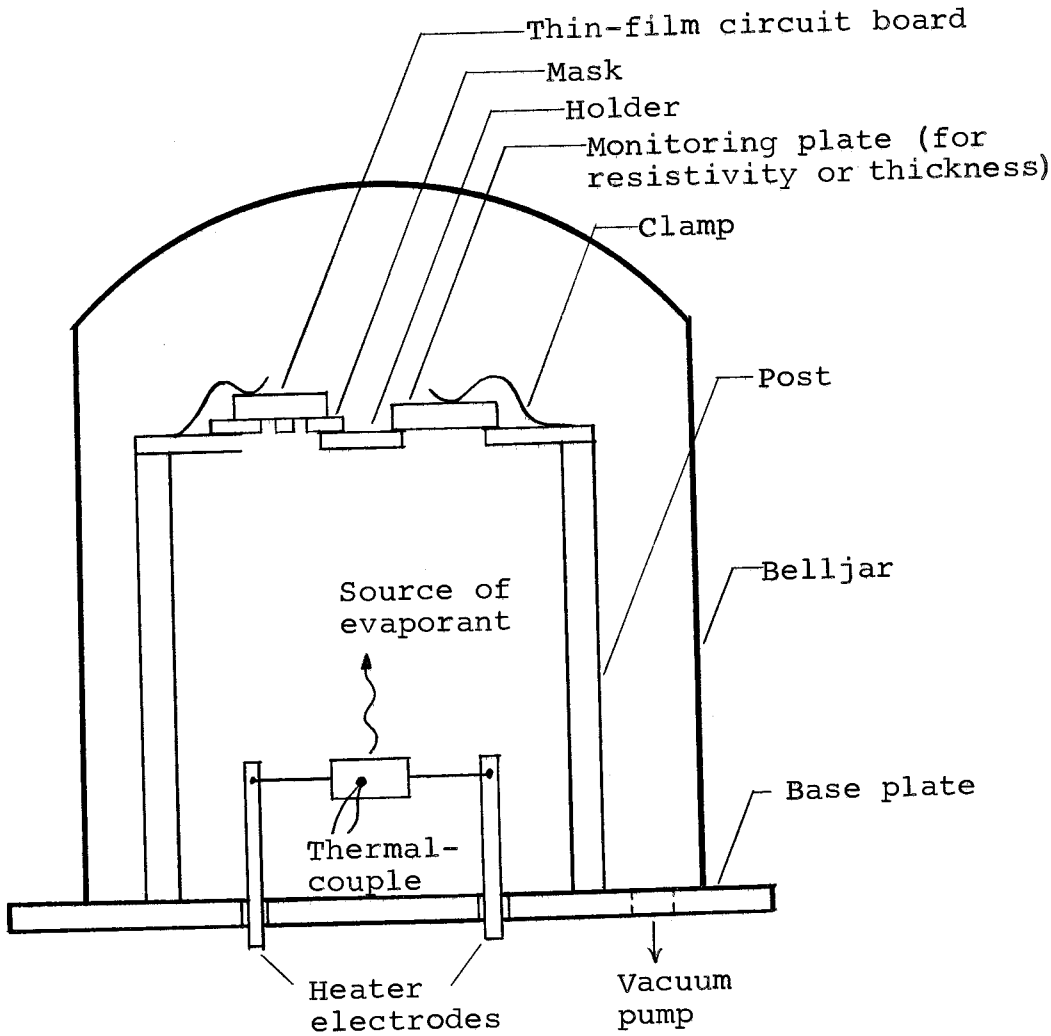

Figure 37. Chamber layout for thin-film depositions.

mechanical linkages are omitted from the drawing for clarity. The pertinent data concerning the evaporation process are given in Table IV.

Considerable difficulty was encountered in constructing the thin-film circuits. The main problem was with the capacitors. Despite the precautions taken in the SiO thin-film deposition, a number of the capacitors in each circuit board invariably were short-circuited to the ground plate. The cause of the short-circuits can be attributed to either the pin-holes in the SiO film or dust on the surface during the evaporation. Neither could be corrected easily in an experimental laboratory. Also, a gross error was involved in the design of the capacitors. The upper plate of a thin-film capacitor should be designed to have a smaller area than the ground plate to avoid short-circuits over the edges (where the SiO film was thinnest) of the capacitor. This step was overlooked in the design.

Instead, time was spent to cure the short-circuited capacitors. High current pulses were applied to the short-circuited capacitors in increasing magnitude until the shorting path (or paths) in the capacitors were burned away. The current source for this operation had an open-circuit voltage less than the breakdown voltage of the capacitors (slightly over 15 volts). Otherwise,

Table IV. Data on the Construction of the Thin-Film Circuit.

Deposition	Pressure[5] (micron)	Heat Source	Source Temp. (°C)	d (inch)	t (Å)	ρ (ohm/sq.)	Remarks
Aluminum (Al)	0.1	Tungsten wire	1100	12	opaque	-	Amount of source material determined film thickness
Silicon Monoxide (SiO)	0.07	Tantalum baffled box[6]	1150	8	5000	-	Sloan[7] deposition thickness monitor used to monitor film thickness
Nichrome Ni/Cr	0.1	Tungsten coil	1200	12	-	20	Resistivity was monitored by employing an additional slide, with electrical contacts. Ohmeter connected to slide gave instantaneous ohm/sq. readings.

d -- distance between depositing surface and evaporant

t -- thickness of film

ρ -- resistivity of film

[5] The vacuum evaporator used was manufactured by Mikros, Inc., Portland, Oregon.

[6] The tantalum baffled box was manufactured by R. D. Mathis Company, Long Beach, California.

[7] The deposition thickness monitor, DTM-3, was manufactured by Sloan Instrument Corporation, Santa Barbara, California.

the capacitors would be destroyed by the power surge once the short-circuits were eliminated.

Most of the short-circuited capacitors were cured by the method mentioned and the circuit boards were saved. However, it was observed that the short-circuits were recurrent with time and the burn-out treatment had to be repeated. This problem persisted throughout the experiment.

Figure 38 shows the completed thin-film curcuit board for a two-stage amplifier. The labels on the photograph correspond to the circuit diagram of the two-stage amplifier shown in Figure 16. Considerable distortion was introduced in the photograph due to the slanting of the slide. The slide was tilted during photographing for proper illumination of the reflective metal surfaces.

The active devices (the transistors and tunnel-diodes) and their leads were fastened down, mechanically as well as electrically, to the thin-film circuit board by conducting glue.[8] The completed two-stage thin-film hybrid circuit is shown in Figure 39.

---

[8] The air dry silver conductive glue, trade named Silver Print, is produced by GC Electronics, Rockford, Illinois.

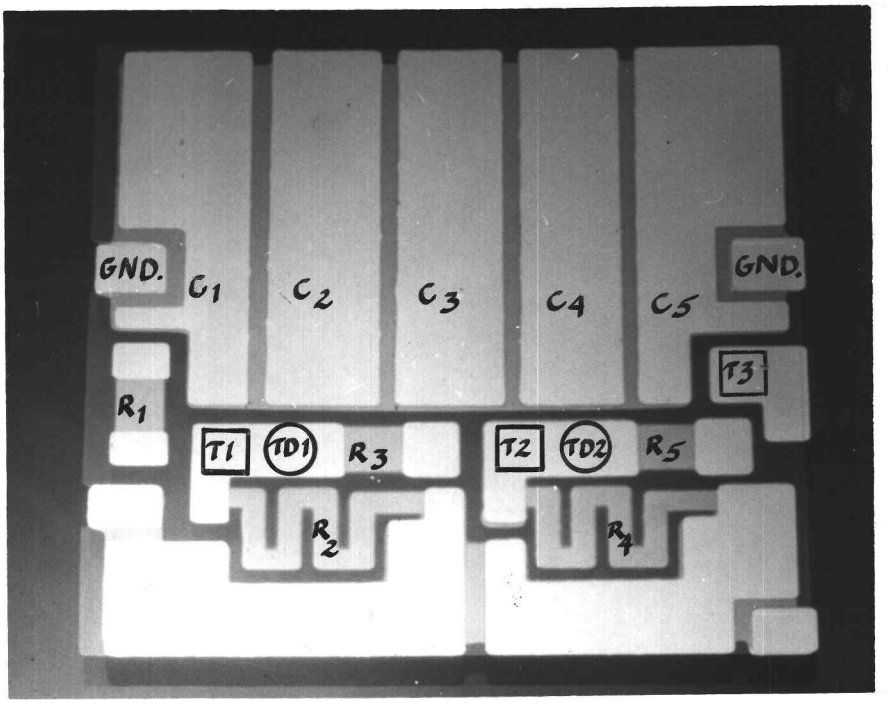

Figure 38. Completed thin-film circuit board for two-stage amplifier (actual size: 6/10 x 6/10 sq. inch).

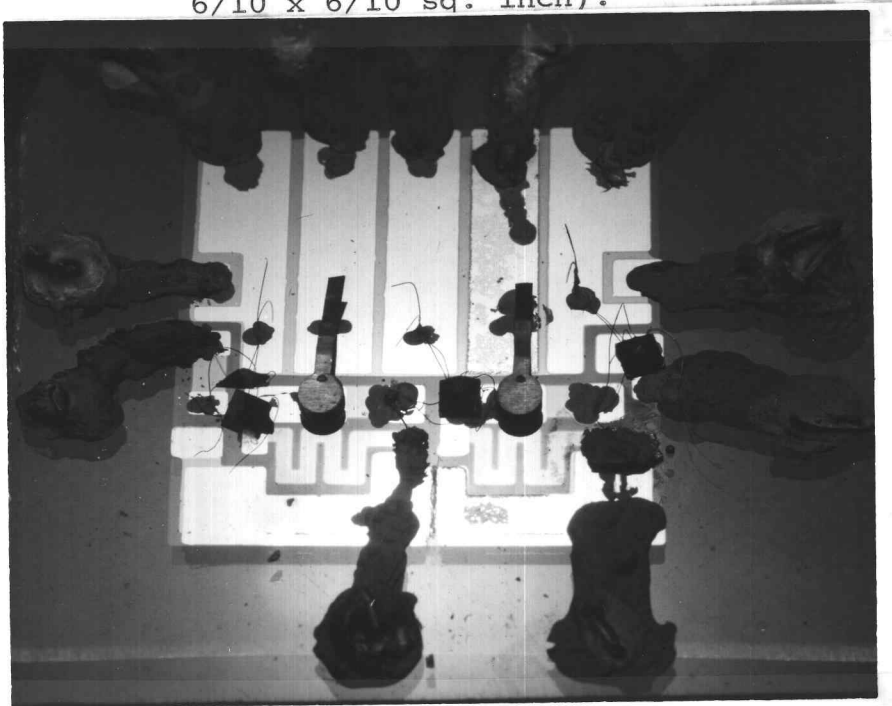

Figure 39. Close-up of the two-stage thin-film hybrid amplifier.